15. Acoustic Communication

Milica Stojanovic, Pierre-Philippe J. Beaujean

In this chapter, we discuss acoustic communication methods which are used to provide wireless connection between remote nodes operating in an underwater environment. We begin with an introductory overview of the history of acoustic communication, and an outline of current and emerging applications. We then provide a summary of communication channel characteristics, with an eye towards acoustic propagation mechanisms and the ways in which they differ from radio propagation. The main focus of our treatment is on two major aspects of communication system design: the physical link and the networking functions. On the physical link level, we discuss noncoherent and coherent modulation/detection methods, paying attention to both single-carrier modulation and multicarrier broadband techniques. Specifically, we discuss signal processing methods for synchronization, equalization, and multichannel (transmit and receive) combining. On the networking level, we discuss protocols for channel sharing using both deterministic division of resources (frequency, time, and code-division multiple access) and random access, and we also overview recent results on routing for peer-to-peer acoustic networks. We conclude with an outline of topics for future research.

Wireless transmission of signals underwater over distances in excess of a 100 m relies almost exclusively on acoustic waves. Radio waves do not propagate well underwater, except at low frequencies and over extremely short distances (a few meters at 10 kHz) [15.1]. Optical signals, which are best used in the blue–green region (around 500 nm), also suffer from attenuation and do not propagate beyond about 100 m, although they do offer high bandwidths (on the order of MHz) [15.2]. Hence, sound is used for wireless transmission over anything but very short distances. Sound propagates as a pressure wave, and it can thus easily travel over kilometers, or even hundreds of kilometers, but to cover a longer distance, a lower frequency has to be used. In general, acoustic communications are confined to bandwidths that are low compared to those used for terrestrial radio communications. Acoustic modems that are in use today typically operate in bandwidths on the order of a few kHz, at a comparably low center frequency (5 centered at 10 kHz) [15.3]. While such frequencies will cover distances on the order of a kilometer, acoustic frequencies in the 100 kHz region can be used for shorter distances, while frequencies below a kHz are used for longer distances. Underwater acoustic communication over basin scales (several thousand kilometers) can be established in a single hop as well; however, the attendant bandwidth will be only on the

order of 10 Hz [15.4]. Horizontal transmission is notoriously more difficult due to the multipath propagation, while vertical channels exhibit less distortion [15.5]. Frequency-dependent attenuation, multipath propagation, and low speed of sound (about 1500 m/s), which results in a severe Doppler effect, make the underwater acoustic channel one of the most challenging communication media.

15.1 A Brief History

Among the first operational underwater acoustic systems was the submarine communication system developed in the United States around the end of the Second World War. This system used analog modulation in the 8–11 kHz band (single-sideband analog modulation AM) [15.6]. Technology has since advanced, pushing digital modulation/detection techniques into the forefront of modern acoustic communications. In the early 1980s, the advent of digital signal processing sparked a renowned interest in underwater acoustic communications, leading a group of scientists at the Massachusetts Institute of Technology and the Woods Hole Oceanographic Institution (WHOI) to propose a system based on frequency shift keying (FSK) [15.7]. The system became known as DATS (digital acoustic telemetry system) and provided a basis for the first generation of commercial digital acoustic modems [15.8]. Today, coded FSK is used in several acoustic modems, including the WHOI *micro-modem* and the Teledyne (formerly Benthos) *telesonar type B* modem [15.9]. While FSK relies on simple energy detection (noncoherent detection), and thus offers robustness to channel impairments, its bandwidth utilization is not efficient. Motivated by this fact, research in the 1990s focused on investigating phase shift keying (PSK) and quadrature amplitude modulation (QAM) for underwater acoustic channels. These modulation methods offer more bits/sec per Hz of occupied bandwidth, but require a receiver that can track the channel and compensate for the time-varying multipath and phase distortion (coherent detection). Work carried out at Northeastern University and WHOI resulted in a channel equalization/synchronization method [15.10], which forms the basis of a second generation of *high-speed* acoustic modems. Through the last decade, these modems have been used in operations involving both stationary platforms and autonomous underwater vehicles (AUVs), over vertical and horizontal links at bit rates of about 5 kbps. [15.11] gives an impressive account of a 2009 deployment near the 11 km deep Mariana Trench. A detailed summary of existing technology is given in Sect. 15.3.

Bit rates in excess of those available with operational modems have been demonstrated as well, but these results are in the domain of experimental research. At the time of this writing, research is active on improved, and ever more sophisticated channel estimation and equalization methods for single-carrier broadband systems, as well as on multicarrier modulation/detection techniques which hold a promise of reducing the implementation complexity of high-speed acoustic modems. The success of various communication techniques largely depends on our understanding of the acoustic communication channel, i. e., our ability to identify a proper model for signal distortion. We thus begin our treatment of acoustic communications links by outlining the channel characteristics in Sect. 15.4, and then move on to discuss the basic as well as the emerging concepts of signal processing in Sect. 15.5.

As technology advances, companies around the world engage more easily in modem development, and the legacy of US manufacturers such as Teledyne-Benthos, WHOI, and Link-Quest are joined by new ones such as the French Thales and the German Evo-Logics. As a result, standardization efforts are becoming necessary to ensure inter-operability between acoustic modems of different manufacturers [15.12]. While it is ultimately the need for a certain technology that will dictate the usefulness of its presence on the market, we must keep in mind that application-driven technology development is not the only way forward. More often than not, technology-driven applications arise – wireless radio industry being the prime example. In other words, as the acoustic modems' capabilities grow, applications that previously were not thought possible may start to emerge.

15.2 Current and Emerging Modem Applications

Modem applications range from ocean observation to the oil industry and aquaculture, and include gathering of sensor data from remote instruments for pollution control, climate recording and prediction of natural dis-

turbances, as well as the detection of objects on the ocean floor, and transmission of images from remote sites. Implicitly, wireless signal transmission is also crucial for monitoring and control of remote instruments, and for communicating with robots and AUVs, which can serve on isolated missions, or as parts of a mobile network. Applications involving AUVs range from search and survey missions to supervisory control and collection of mapping data, be they images, video, or side-scan sonar.

Autonomous systems are envisioned both for stand-alone applications and as wireless extensions to cabled systems. For example, a stand-alone 15 kbps acoustic link, intended to provide data transfer from bottom-mounted, battery-powered instruments such as seismometers to a surface buoy is described in [15.5]. A different example is that of ocean observatories, which are being built on decommissioned submarine cables to deploy an extensive fiber optic network of sensors (cameras, wave sensors, seismometers) covering miles of ocean floor [15.13]. These cables can also carry communication access points, very much as cellular base stations are connected to the telephone network, allowing users to move and communicate from places where cables cannot reach. Another example are cabled submersibles, also known as remotely operated vehicles (ROVs). These vehicles, which may weigh more than 10 metric tons, are connected to a mother-ship by a cable that can extend over several kilometers and deliver high power to the remote end, along with high-speed communication signals. A popular example of an ROV/AUV tandem is the WHOI's Alvin/Jason pair of vehicles that were deployed in 1985 to discover the Titanic. Such vehicles were also instrumental in the discovery of hydro-thermal vents, sources of extremely hot water on the bottom of deep ocean, which revealed forms of life different from any others known previously. The first vents were found in the late 1970s, and new ones are still being discovered. The importance of such discoveries is comparable only to space missions, and so is the technology that supports them. Today, vehicle technology, sensor technology, and acoustic communication technology are mature enough to support the visionary idea of an autonomous oceanographic sampling network [15.14]. Recent years have seen a proliferation of research on underwater sensor networks, which we discuss in Sect. 15.5.6.

15.3 Existing Technology

The field of underwater acoustic communication has become fairly mature. Many commercial units are available, along with a significant number of prototypes developed in research laboratories. The large number of configurations available complicates the selection process of a specific underwater acoustic modem. The purpose of this section is to offer some guidance in selecting an underwater acoustic modem. The authors do not recommend any specific product, rather they highlight what is important in the selection process. Following this, a brief overview of typical performance and field tests is presented.

15.3.1 System Requirements

Underwater acoustic modem users should always keep in mind that the performance of these systems changes dramatically depending on the application. For example, a system designed to operate at tens of kilometers will typically have a much lower throughput than a system designed to relay data at a few hundred meters. Also, some underwater acoustic modems are designed to operate in a complex network, while others are designed for point-to-point communication between two units.

The following list is by no mean exhaustive, but covers the main factors that should be used in selecting an underwater acoustic modem:

- *Application*: The user should always keep the application in mind when selecting an acoustic modem. Voice communication constitutes a category of its own, with well-proven technology specifically designed to relay intelligible voice with minimal delay and simultaneous two-way communication capability. Acoustic modems designed for the transmission of command-and-control messages operate more slowly, but very reliably. Image streaming can be achieved using the latest generation of high-bit rate (one-way) acoustic modems. Voice communication modems and command-and-control modems technology is much more mature than image streaming modems.
- *Cost*: Typically between $5,000 and $50,000 (US) per unit, depending on the complexity and performance.
- *Size*: Underwater acoustic modems are usually cylindrical in shape, with a pressure vessel containing the electronics and one or multiple transducers mounted on one end. The size varies from 0.05 m

diameter by 0.1 m in length, to 0.1 m in diameter by 0.5 m in length, depending on the frequency of operation (from a few to hundreds of kHz), maximum range and operating depth.

- *Power*: The power consumption depends on the range and modulation: traditionally, the total power consumption is of the order of 0.1−1 W in receive mode (depending on the receiver complexity), and 10−100 W in continuous transmission mode.
- *Data rate*: (1) underwater acoustic modems designed to operate very reliably in challenging environments, on moving platforms and over distances of several kilometers typically operate under 1000 bps; (2) in less challenging environments (e.g., vertical communications in deep waters), acoustic modems can operate at data rates well over 1000 bps.
- *Horizontal versus vertical transmission*: It is critical to understand that commercial underwater acoustic modems come in different versions depending on the type of operation. In particular, acoustic modems designed for vertical transmission in deep water use directional transducers and are capable of high data rates. A traditional mistake is to purchase this type of acoustic modems for horizontal transmission in shallow water, especially on moving platforms; in this case, acoustic modems with omnidirectional and a lower data rates should be selected.
- *Shallow water versus deep water communications (horizontal or slanted)*: In deep waters, fluctuations in sound speed (caused by changes in temperature, hydrostatic pressure, and chemical content) change the direction of propagation of sound (a phenomenon known as sound refraction). This often results in shadow zones: the sound produced by a modem will not reach the other modem, even if both modems are within operating range of one another. Echoes reflected off the sea surface and sea bottom may also be an issue at low frequencies, along with the presence of thermoclines or thermohalines. In shallow waters, the main source of limitation fades, which results from the many echoes reflected off the sea surface and sea bottom. As a result, underwater acoustic modems designed to operate in shallow waters are less likely to be in a shadow zone, but the received signal is often badly distorted and requires specific signal processing techniques (equalization, spread spectrum signaling, power, error coding) to operate reliably.
- *Range*: for the most part, the maximum operational range of an underwater acoustic modem depends on the operating frequency band of the acoustic modem, power, signaling (modulation, error coding, equalizing), environment, and transducer directivity. At low frequencies (a few kHz), commercial acoustic modems achieve reliable acoustic communications beyond 10 km horizontally, albeit at a low data rate (less than 400 bps). As frequency and bandwidth increases, some acoustic modems can transmit data at 10,000 bps or more, but the practical range is limited to 1000 m or less.
- *Operations in dynamic environments*: (1) surface activity causes Doppler spread, which limits the data rate and reliability; (2) platform dynamics cause Doppler shift, which limits the acoustic modem performance when excessive. Moving platforms usually require the use of omnidirectional transducers to avoid loss of acoustic communication.
- *Protocol for point-to-point quality of service* (*QoS*): reliability, delay, retransmission.
- *Networking capability*: Most acoustic modems are designed for point-to-point operation using a point-to-point protocol (PPP). Some series are also designed to support multiple access (MA), where two or more units can be operated within the same environment. In this case, the acoustic modems are usually operated sequentially and can be taken in and out of the water with minimal disruption to the other units. The most sophisticated acoustic modem now support routing capability between nodes, although this feature is rarely available commercially. In this case, one or more acoustic modems can operate together to relay messages over longer distances.
- *Compatibility requirements*: Interoperability between underwater acoustic modems produced by various manufacturers is still work in progress. Protocols and standards exist, but every manufacturer uses its own proprietary modem signaling and protocol. As a result, mixing and matching acoustic modems from different manufacturers is not recommended.

15.3.2 Commercially Available Modems

Figure 15.1 provides an overview of the nominal data rate versus range resulting from a large literature survey. In general, the high rate or high range results are for deep channels while the cluster of low range, low rate are for shallow channels. Modems developed by the research community are represented with diamonds, while stars denote commercially available systems. The range-times-rate bound represents an estimate of the existing performance envelope. While there are exceptions, most reviewed systems are bounded by this performance limit. Table 15.1 and Fig. 15.2 provide a few examples of state-of-the-art acoustic modems. The information is obtained from published technical specifications. Every acoustic communication system

Table 15.1 A few acoustic modems

Product name	Max bit rate [bps]	Range [m]	Frequency band [kHz]
Teledyne Benthos ATM-916-MF1 [15.15]	15360	6000	16–21
WHOI Micromodem [15.16]	5400	3000	22.5–27.5
Linkquest UWM 1000 [15.17]	7000	1200	27–45
Evologics S2C R 48/78 [15.18]	31200	2000	48–78
Sercel MATS 3G 34 kHz [15.19]	24600	5000	30–39
L3 Oceania GPM-300 [15.20]	1000	45000	not specified
Tritech Micron Data Modem [15.21]	40	500	20–28
FAU Hermes [15.22]	87768	180	262–375

presented here is of excellent quality and reputation and uses field-tested technologies. This short section cannot provide a complete description of the acoustic communications field. Many other acoustic communication systems have been developed over the past three decades that could not be included due to space limitations. Because underwater acoustic modems are very specialized pieces of equipment produced in limited numbers, standardizing hardware and protocols is a work in progress. Although most developers and manufacturers use proprietary hardware and protocols, a compact control language [15.23] has been developed to make optimal use of the limited acoustic modem data throughput installed on unmanned underwater vehicles. In addition, three frequency bands, common between a large number of underwater acoustic modems, have been identified. Finally, some efforts have been made in developing some level of inter-operability between underwater acoustic modems produced by different manufacturers. Although these efforts are encouraging, combining devices originating from different companies in the same network is usually not desirable.

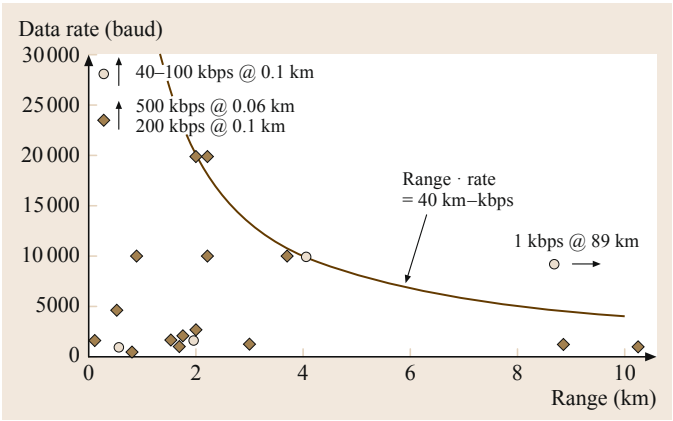

Fig. 15.1 Published experimental performance of underwater acoustic telemetry systems is summarized in this plot of rate [kbps] versus range [km] (after [15.24]). The channels vary from deep and vertical to shallow and horizontal

15.3.3 Field Tests

Field testing is a key step in evaluating the performance of an underwater acoustic communication system. Because of the extensive cost of such tests (especially in deep waters), numerous numerical models have been developed to predict the system performance and reduce the required in-water time for test and evaluation.

Underwater acoustic wave propagation is a complex combination of energy dissipation due to viscosity and chemical reactions, fluid–structure interaction, surface wave activity, biological activity, boat traffic, and source and receiver characteristics [15.25, 26]. The acoustic channel characteristics change with time, spa-

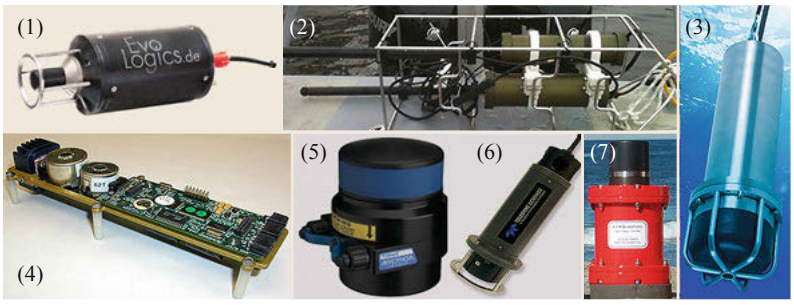

Fig. 15.2 A few examples of state-of-the-art underwater acoustic modems: (1) Evologics S2C R 48/78 (after [15.18]); (2) FAU Hermes (after [15.22]); (3) Sercel MATS 3G 34 kHz (after [15.19]); (4) WHOI Micromodem (after [15.16]); (5) Tritech Micron Data Modem (after [15.21]); (6) Teledyne Benthos ATM-916-MF1 (after [15.15]); (7) Linkquest UWM 1000 (after [15.17])

tial location, and frequency. The accurate representation of such a complex and dynamic system at any time, location, and frequency is simply not possible. As a result, even the most sophisticated models often display significant difference with measurements. Significant efforts are made to adapt the statistical models developed for radio communications, but much work remains in making these models sufficiently accurate.

Various scientific and governmental organizations (spearheaded by the United States Office of Naval Research), have developed series of comparative tests for existing technology and signal waveforms (Signal-ex, Modem-ex, KAM'11 [15.27]) and underwater acoustic networks (e.g., SeaWeb [15.28]). One key benefit of such tests is the careful monitoring of environmental characteristics during the test.

15.4 Propagation Channel

15.4.1 Attenuation and Noise

A distinguishing property of acoustic channels is the fact that the path loss depends on the signal frequency. This dependence is a consequence of absorption, i. e., transfer of acoustic energy into heat. In addition to the absorption loss, signal experiences a spreading loss which increases with distance. The overall path loss is given by [15.29]

$$A(l,f) = (l/l_{\text{ref}})^k \mathrm{a}(f)^{l-l_{\text{ref}}} , \tag{15.1}$$

where f is the signal frequency and l is the transmission distance, taken in reference to some l_{ref}. The path loss exponent k models the spreading loss, and its usual values are between 1 and 2, for cylindrical and spherical spreading, respectively. The absorption coefficient can be expressed empirically, using Thorp's formula, which gives $\mathrm{a}(f)$ in dB/km for f in kHz as [15.29]

$$10\log \mathrm{a}(f) = 0.11\frac{f^2}{1+f^2} + 44\frac{f^2}{4100+f^2} + 2.75\cdot 10^{-4} f^2 + 0.003 . \tag{15.2}$$

This formula is generally valid for frequencies above a few hundred Hz. The absorption coefficient is shown in Fig. 15.3. It increases rapidly with frequency, thus imposing a limit on the operational bandwidth that can be used for an acoustic link of a given distance.

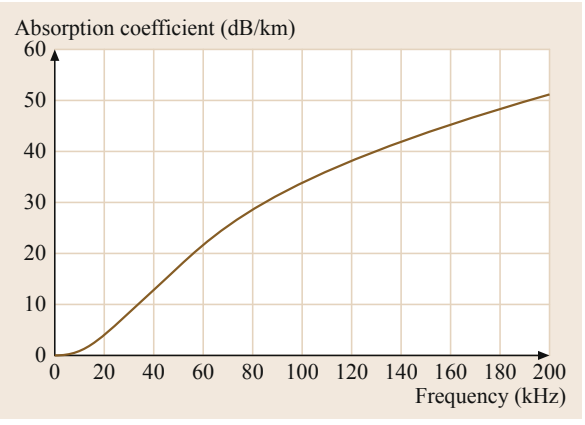

Fig. 15.3 Absorption coefficient, $10\log \mathrm{a}(f)$ in dB/km

Noise in an acoustic channel consists of ambient noise and site-specific noise. Ambient noise is always present in the background of the quiet deep sea. Site-specific noise, on the contrary, exists only in certain places. For example, ice cracking in polar regions creates acoustic noise, and so does shrimp snapping in tropical waters. Ambient noise comes from sources such as turbulence, distant shipping, and breaking waves, in addition to thermal noise. While this noise may be approximated as Gaussian, it is not white. The power spectral density (PSD) of the four noise components is given by the following empirical formulae in dB re μ Pa per Hz as a function of frequency in kHz

$$\begin{aligned} 10\log N_t(f) &= 17 - 30\log f \\ 10\log N_s(f) &= 40 + 20(s-0.5) + 26\log f \\ &\quad - 60\log(f+0.03) \\ 10\log N_w(f) &= 50 + 7.5w^{1/2} + 20\log f \\ &\quad - 40\log(f+0.4) \\ 10\log N_{th}(f) &= -15 + 20\log f . \end{aligned} \tag{15.3}$$

Figure 15.4 shows the total PSD of the ambient noise for several values of the wind speed w (wind drives the surface waves which break and generate noise) and several levels of the distant shipping activity $s \in 0, 1]$ (thousands of ships are present in the ocean at any time, and they generate distant noise, which is to be distinguished from the site-specific noise of vessels passing nearby). The noise PSD decays at a rate of approximately 18 dB/decade, as shown by the straight dashed line in Fig. 15.4. This line represents an approximate model for the noise PSD, $N(f) = N_0 \cdot (f/f_{\text{refx}})^{-\eta}$. The parameters N_0 and η can be fitted from the model, but also from the measurements taken at a particular site.

The attenuation, which grows with frequency, and the noise whose PSD decays with frequency, result in a signal-to-noise ratio (SNR) that varies over the signal

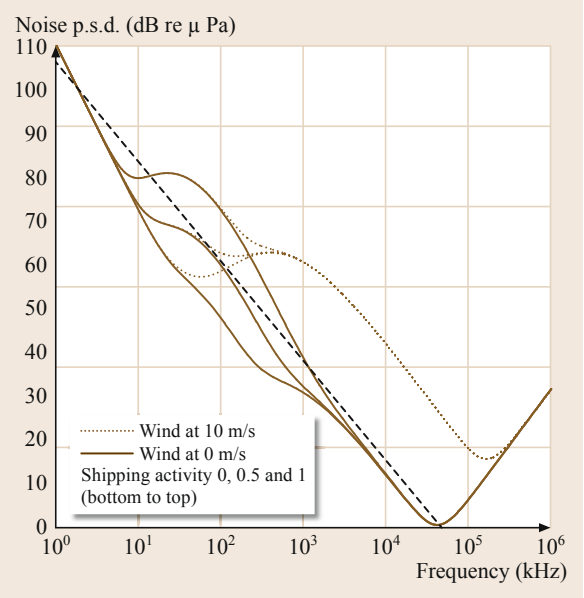

Fig. 15.4 Power spectral density of the ambient noise. The *dash-dotted* line shows an approximation $10\log N(f) = 50\,\text{dB re}\mu\text{Pa} - 8\log(f/1\,\text{kHz})$

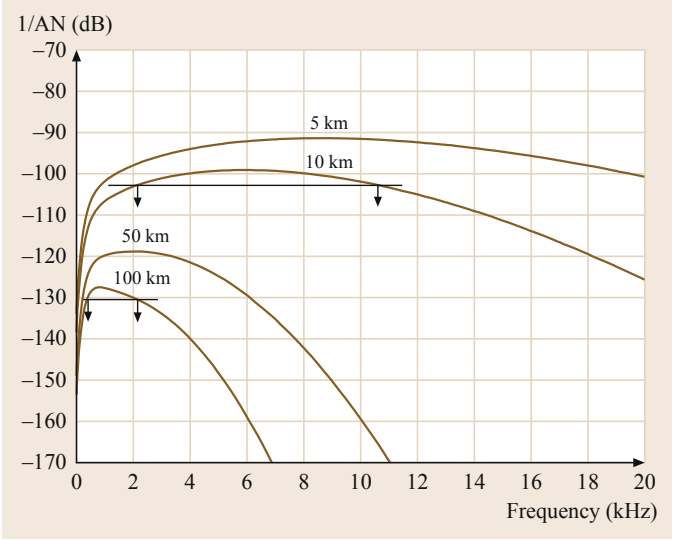

Fig. 15.5 Signal-to-noise ratio in an acoustic channel depends on the frequency and distance through the factor $1/A(l,f)N(f)$. This figure refers to the nominal SNR value that does not include variations induced by shadowing or multipath propagation

bandwidth. If one defines a narrow band of frequencies of width Δf around some frequency f, the SNR in this band can be expressed as

$$SNR(l,f) = \frac{S_l(f)\Delta f}{A(l,f)N(f)\Delta f}\,, \tag{15.4}$$

where $S_l(f)$ is the PSD of the transmitted signal. For any given distance, the narrowband SNR is thus a function of frequency, as shown in Fig. 15.5. From this figure it is apparent that the acoustic bandwidth depends on the transmission distance. In particular, the bandwidth and the power needed to achieve a prespecified SNR over some distance can be approximated as $B(l) = b \cdot l^{-}$ and $P(l) = p \cdot l^{\psi}$, where the coefficients b, p, and the exponents $\in (0,1), \psi \geq 1$, depend on the target SNR, the parameters of the acoustic path loss, and the ambient noise [15.30]. The bandwidth is severely limited at longer distances: at 100 km, only about a kHz is available. At shorter distances, the bandwidth increases, but it will ultimately be limited by that of the transducer. The fact that the bandwidth is limited implies the need for bandwidth-efficient modulation methods if more than a bps/Hz is to be achieved over these channels.

Another important observation to be made is that the acoustic bandwidth B is often on the order of the center frequency f_c. This fact bears significant implications on the design of signal processing methods, as it prevents one from making the narrowband assumption, $B << f_c$, on which many radio communication principles are based. Respecting the wideband nature of the system is particularly important in multichannel (array) processing and in synchronization for mobile acoustic systems.

Finally, the fact that the acoustic bandwidth depends on the distance has important implications on the design of underwater networks. Specifically, it makes a strong case for multihopping, since dividing the total distance between a source and destination into multiple hops enables transmission at a higher bit rate over each (shorter) hop. Since multihopping also ensures lower total power consumption, its benefits are doubled from the viewpoint of energy-per-bit consumption on an acoustic channel [15.31]. Granted, by increasing the number of hops, the level of interference will increase, and packet collisions may become more likely, requiring, in turn, more re-transmissions. However, as shorter hops support higher bit rates, data packets containing a given *number* of bits will have shorter *duration* if the bit rate is appropriately increased, and the chances of collision will be reduced. This fact speaks further in favor of acoustic system design based on high-bandwidth, multihop links.

15.4.2 Multipath Propagation

While the basic propagation loss describes energy spreading and absorption, it does not take into account the specific system geometry and the resulting multipath propagation. Multipath formation in the ocean is

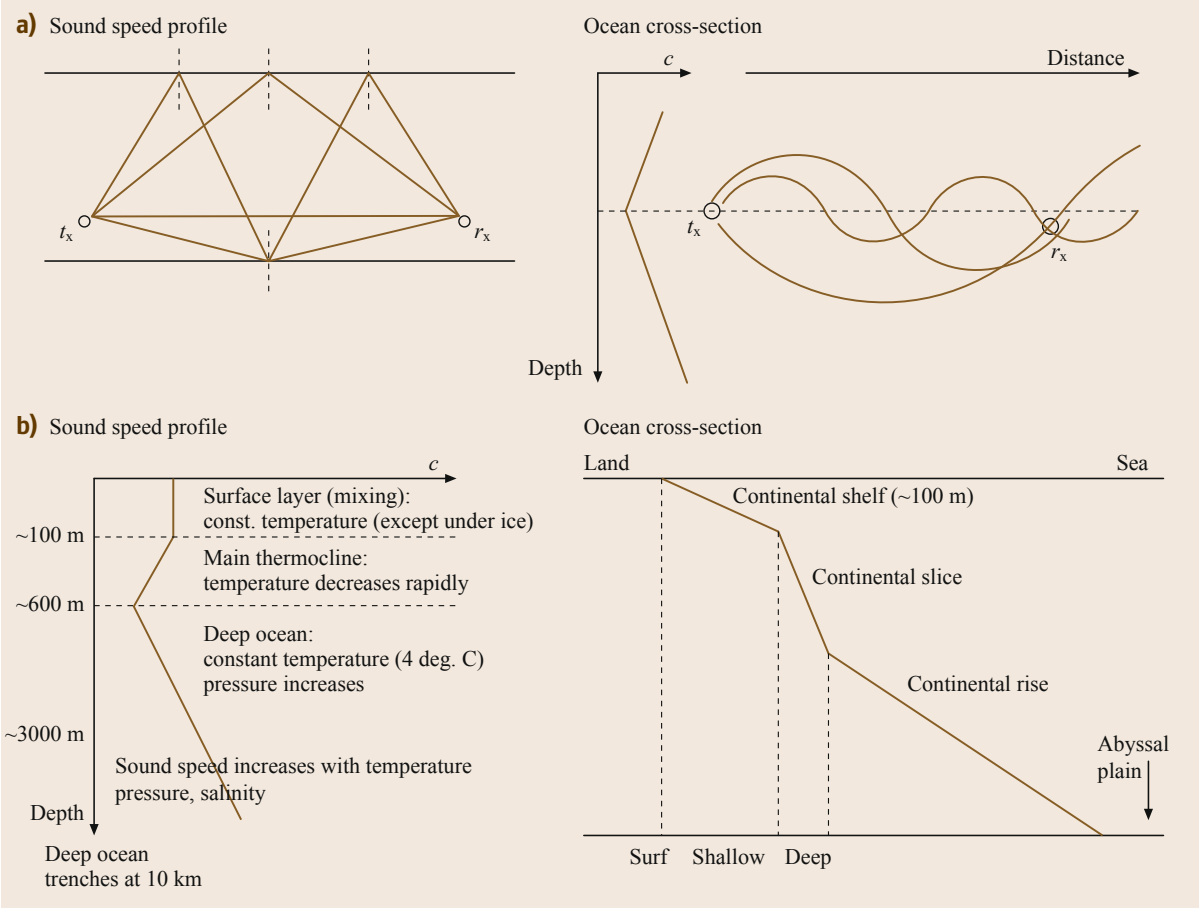

Fig. 15.6a,b Multipath formation in shallow and deep water **(a)**. Sound speed as a function of depth and the corresponding ocean cross-section **(b)**

governed by two effects: sound reflection at the surface, bottom and any objects, and sound refraction in the water. The latter is a consequence of sound speed variation with depth, which is mostly evident in deep water channels. Figure 15.6 illustrates the two mechanisms.

Sound speed depends on the temperature and pressure, which vary with depth, and a ray of sound always bends towards the region of lower propagation speed, obeying Snell's law. In shallow water, both the temperature and the pressure are constant, and so is the sound speed. As the depth increases, the temperature starts to decrease, but the weight of the water above is still not significant enough to considerably change the pressure. The sound speed thus decreases in the region called the main thermocline. After a certain depth, the temperature reaches the constant level of 4 C, and from there on the sound speed increases with pressure. When a source launches a beam of rays, each ray will follow a slightly different path, and a receiver placed at some distance will observe multiple signal arrivals. Note that a ray traveling over a longer path may do so at a higher speed, thus reaching the receiver before a direct, stronger ray. This phenomenon results in a nonminimum-phase channel response.

The first approach to modeling multipath propagation is a deterministic one, which provides an exact solution for the acoustic field strength in a given system geometry with a given sound speed profile. Because of computational complexity, approximate solutions are often used instead of the exact ones. An approximation that is suitable for frequencies of interest to acoustic communication systems is based on ray tracing. A widely-used package, Bellhop, is available online [15.32] (see also [15.33, 34]). Figure 15.7 illustrates a ray-trace obtained for a transmitter placed inside the circle to the left. Lighter colors in this figure indicate locations of higher received signal strength. If a receiver is placed at some distance away from the transmitter in this field, the signal strength will vary depending upon the *exact* location. In other words, two receivers (e.g., two circles to the right) placed at the *same* distance away from the transmitter, may experi-

ence propagation conditions that are quite different. In this example, shadowing is caused by ray bending in deep water. In shallow water with constant sound speed, signal strength can be calculated using simple geometrical considerations. Alternating constructive/destructive combining of multiple reflections will now form pockets of strong/weak signal reception. In either case, multipath effects make the signal strength location dependent, i. e., different from the value predicted by the basic propagation loss (15.1). If the transmitter or receiver were to move through this frozen-in-time acoustic field, the received signal strength would be perceived as varying. In practice, of course, neither the channel geometry nor the environmental parameters are frozen, and small disturbances cause the signal strength to vary in time even if there is no intentional motion of the transmitter or receiver.

The impulse response of an acoustic channel is thus influenced by the geometry of the channel and its reflection and refraction properties, which determine the number of significant propagation paths, their relative strengths and delays. Strictly speaking, there are infinitely many signal echoes, but those that have undergone multiple reflections and lost much of the energy can be discarded, leaving only a finite number of significant paths.

To put a mathematical channel model in perspective, let us denote by $\bar{l}_p$ the nominal length of the p-th propagation path, with $p = 0$ corresponding to a reference path (either the strongest, or the first significant arrival). In shallow water, where the sound speed c can be taken as constant, path delays can be obtained as $\bar{\tau}_p = \bar{l}_p/c$. The surface reflection coefficient equals -1 under ideal conditions, while bottom reflection coefficients depend on the type of bottom (hard, soft) and the grazing angle [15.35]. If we denote by Γ_p the cumulative reflection coefficient along the pth propagation path, and by $A(\bar{l}_p, f)$ the propagation loss associated with this path, then

$$\overline{H}_p(f) = \frac{\Gamma_p}{\sqrt{A(\bar{l}_p, f)}} \tag{15.5}$$

represents the nominal frequency response of the p-th path. Hence, *each path* of an acoustic channel acts as a low-pass filter. Figure 15.8 illustrates a reference path transfer function $\overline{H}_0(f) = 1/\sqrt{A(\bar{l}_0, f)}$.

For the distances and frequencies of interest to the majority of acoustic communication systems, the effect of path filtering is approximately the same for all paths, as the absorption coefficient does not vary much from its value at the reference distance and center frequency. Denoting this value by a_0, the transfer function of the

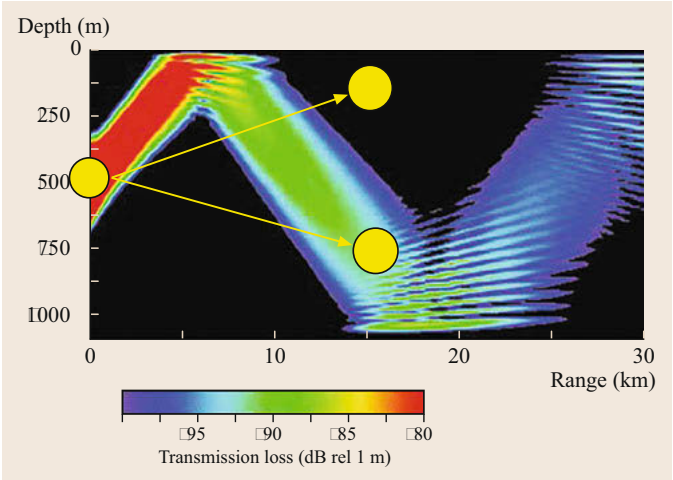

Fig. 15.7 A ray-trace shows areas of strong/weak signal reception. Sound reflection and refraction result in multipath propagation which favors some locations while placing others in a shadow

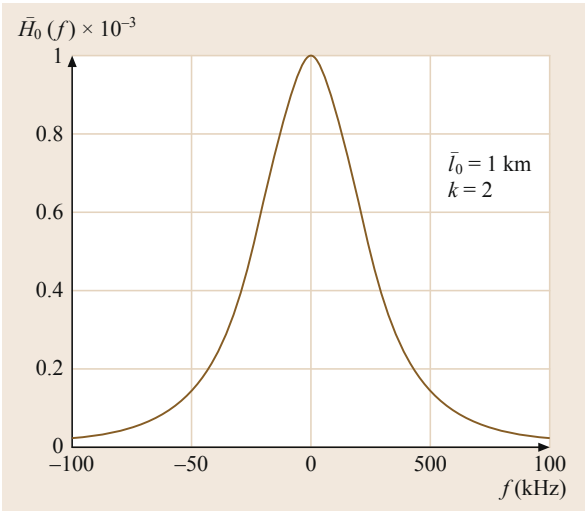

Fig. 15.8 Example of a reference path transfer function $\overline{H}_0(f)$

p-th path is modeled as

$$\overline{H}_p(f, t) = \overline{h}_p \cdot \overline{H}_0(f) \,, \tag{15.6}$$

where

$$\overline{h}_p = \frac{\Gamma_p}{\sqrt{(\bar{l}_p/\bar{l}_0)^k a_0^{\bar{l}_p - \bar{l}_0}}} \tag{15.7}$$

is the real-valued (passband) path gain. Figure 15.9 shows an example of nominal multipath structure.

In an acoustic communication system, the channel can be observed only in a limited band of frequencies supported by the transducer. As a result, the observable response will be smeared, as illustrated in Fig. 15.10.

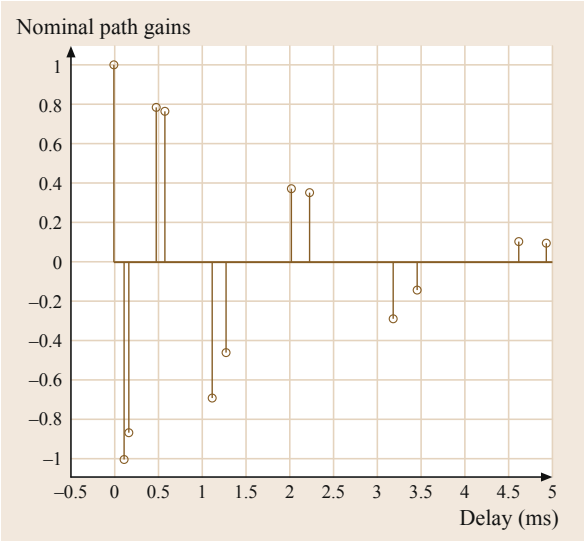

Fig. 15.9 Nominal path gains (15.7) for a channel with transmission distance $d = 1\,\text{km}$, water depth $h = 20\,\text{m}$, and transmitter/receiver height above the bottom $h_T = 10\,\text{m}$ and $h_R = 12\,\text{m}$. The surface reflection coefficient is -1; bottom reflection coefficients are calculated assuming speed of sound and density of $c = 1500\,\text{m/s}$, $\rho = 1000\,\text{kg/m}^3$ in water and $c_b = 1300\,\text{m/s}$, $\rho_b = 1800\,\text{kg/}m^3$ in the soft bottom. Those paths whose absolute value is above one tenth of the strongest path's are shown

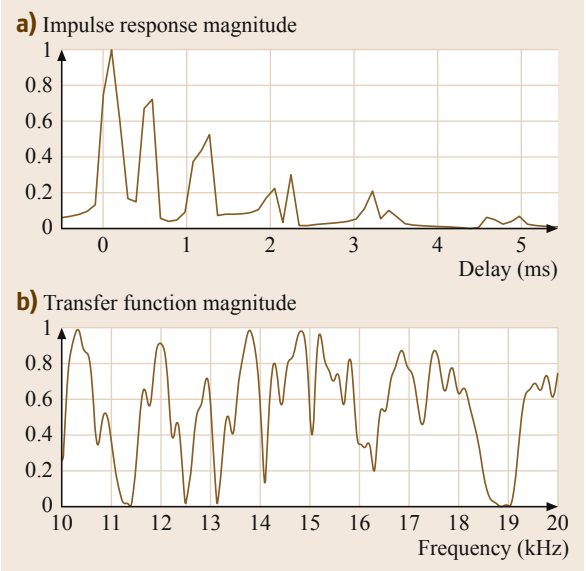

Fig. 15.10 **(a)** Impulse response (baseband) and **(b)** the transfer function for the nominal (time-invariant) channel geometry corresponding to the multipath structure of Fig. 15.9, as seen in $B = 10\,\text{kHz}$ of bandwidth centered at $f_c = 15\,\text{kHz}$. In a wideband acoustic system, multipath propagation creates discernible signal echoes and a frequency-selective channel distortion

It is important to make the distinction between the natural channel *paths* of the channel (Fig. 15.9), and the samples of the observable response (Fig. 15.10). The latter are often referred to as the channel *taps*. It is also important to note that the path gains can be very stable, while taps may exhibit fast variation. Such behavior is explained by the fact that each tap contains contributions from *all* the paths, wherein each path carries a pulse of finite duration and a different delay that varies in time. An example of tap variation is shown in Fig. 15.13, which we will discuss later when we address channel fading.

Multipath propagation creates a frequency-selective channel distortion, which is evident as the variation of the transfer function in Fig. 15.10. As a result, some frequencies of a wideband acoustic signal will be favored, while others will be severely attenuated. Channel equalization has to be employed to deal with this type of distortion.

The total delay spread between significant multipath arrivals or the *multipath spread* of the channel, T_{mp}, is an important figure of merit for the design of acoustic communication systems. Vertical links exhibit short multipath spreads, while horizontal channels exhibit multipath spreads that can range between a few milliseconds and hundreds of milliseconds. In single-carrier broadband systems, where the data symbols are short compared to the multipath spread, the meaningful figure of merit is the number of symbols that fit within the multipath spread. This number determines the extent of inter-symbol interference (ISI), which in turn dictates the length of the filters needed to equalize the channel. The fact that the multipath spread may be on the order of several milliseconds, or more, implies that the ISI may span tens or even a hundred symbol intervals; a situation very different from that typically found in radio systems, where ISI may involve a few symbols only. Multicarrier systems avoid this problem by transmitting in parallel on many carriers, each occupying a narrow subband. A meaningful figure of merit for these systems is the frequency coherence, $\Delta f_{\text{coh}} = 1/T_{\text{mp}}$. In a properly designed multicarrier system, carrier separation is kept well below this value.

The acoustic channel is often *sparse*, i. e., there are only several significant paths that populate the *total* and possibly long delay spread. This fact has an important implication on channel estimation and the associated equalization methods. Namely, while the entire multipath spread is represented by $L \approx T_{\text{mp}}B$ samples taken at intervals $T_s = 1/B$, fewer than L coefficients may suffice to represent the channel response. Ideally, only as many coefficients as there are propagation paths, $P < L$,

are needed. Channel modeling thus becomes an important aspect of signal processing, and sparsing has been investigated for decision-feedback equalization [15.36, 37], turbo equalization [15.38, 39], and multicarrier detection [15.40–42]. It is also important to note that although a greater bandwidth implies more ISI and more frequency selectivity, it also implies a better resolution in delay (less smearing in the observable channel response). Hence, although the attendant signal distortion is perceived as more severe, channel estimation will be more efficient if a proper sparse model is used, which may, in turn, lead to improved signal processing. In addition, signaling at a higher rate enables more frequent channel observations and, consequently, easier channel tracking [15.43].

15.4.3 Time Variability: Motion-Induced Doppler Distortion

There are two sources of the channel's time variability: inherent changes in the propagation medium, which contribute to signal fading, and those that occur because of the transmitter/receiver motion and contribute to the frequency shifting. The distinction between the two types of distortions is that the first one appears as random, while the motion-induced Doppler effects can be modeled in a deterministic manner and, therefore, compensated to some degree through synchronization.

Motion of the transmitter, receiver, or a reflection point along the signal path causes the path distances to vary with time. The resulting Doppler effect is evident as time compression/dilation of the signal, which causes frequency shifting and bandwidth spreading/shrinking. The magnitude of the Doppler effect is proportional to the ratio $a = v/c$ of the relative transmitter-receiver velocity to the speed of sound. Because the speed of sound is very low as compared to the speed of electromagnetic waves, motion-induced Doppler distortion of an acoustic signal can be extreme. AUVs move at speeds that are on the order of a few m/s, but even without intentional motion, underwater instruments are subject to drifting with waves, currents, and tides, which may occur at comparable velocities. In other words, there is always *some* motion present in the system, and a communication system has to be designed taking this fact into account. The only comparable situation in radio communications occurs in low Earth orbiting (LEO) satellite systems, where the relative velocity of satellites flying overhead is extremely high (the channel there, however, is not nearly as dispersive in delay). The major implication of motion-induced distortion is on the design of synchronization algorithms.

To model the Doppler distortion, let us focus on a single propagation path, assuming that the relative transmitter/receiver velocity v_p along this path stays constant over some interval of time. The path delay can then be modeled as

$$\overline{\tau}_p(t) = \overline{\tau}_p - a_p \cdot t \,, \tag{15.8}$$

where $a_p = v_p/c$ is the Doppler factor corresponding to the p-th path. If there is a single dominant component of velocity, these factors can be approximated as equal for all paths, $a_p = a, \forall p$; however, this is not the case in general [15.37]. To assess the effect of time-varying delay on the signal, let us focus on a particular signal component centered around frequency f_k in a narrow band $\Delta f \ll f_k$. The signal $s_k(t)$ and its equivalent baseband $u_k(t)$ are related by

$$s_k(t) = Re\{u_k(t)e^{i2\pi f_k t}\} \,. \tag{15.9}$$

Since the signal occupies only a narrow band of frequencies, its replica received over the p-th propagation path is given by

$$s_{k,p}(t) = \overline{h}_p \bar{H}_0(f_k) s_k(t - \overline{\tau}_p(t)) \,. \tag{15.10}$$

Defining the equivalent baseband component of the received signal via

$$s_{k,p}(t) = Re\{v_{k,p}(t)e^{i2\pi f_k t}\} \,, \tag{15.11}$$

we have the baseband relationship

$$v_{k,p}(t) = \overline{c}_{k,p} e^{i2\pi a_p f_k t} u_k(t + a_p t - \overline{\tau}_p) \,, \tag{15.12}$$

where

$$\overline{c}_{k,p} = \overline{h}_p \overline{H}_0(f_k) e^{-i2\pi f_k \overline{\tau}_p} \,. \tag{15.13}$$

The Doppler effect is evident in two factors: (i) frequency shifting by the amount $a_p f_k$ and (ii) time scaling by the factor $(1 + a_p)$. The situation of putting together all the signal components at frequencies f_0, f_1, etc., that span a wide bandwidth $B = K\Delta f$, and assuming only a single propagation path with the Doppler factor a is illustrated in Fig. 15.11. This figure offers an exaggerated view of the Doppler effect, but nonetheless one that illustrates the point: each spectral component in a wideband mobile acoustic system is shifted by a *different* amount, and the total bandwidth B is spread over $B(1 + a)$, i. e., a signal of duration T is observed at the receiver as having duration $T/(1 + a)$.

The way in which these distortions affect signal detection depends on the actual value of the factor a. For comparison, let us look at a highly mobile radio system: at 160 km/h (100 mph), $a = 1.5 \cdot 10^{-7}$. This value is low enough that compression/dilation can be neglected.

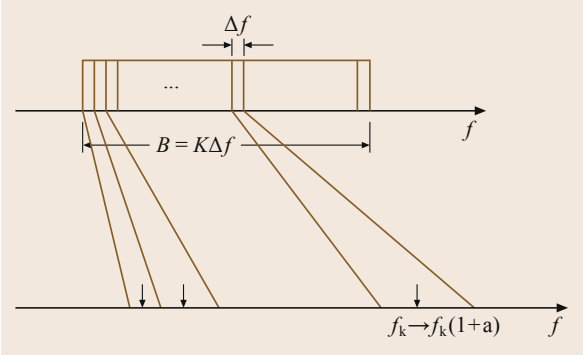

Fig. 15.11 Motion-induced Doppler shift is not uniform in a wideband acoustic system

In other words, there is no need to account for it explicitly in symbol synchronization. The error made in doing so is only 10^{-3} of a bit per 10 000 bit. In contrast to this situation, a stationary acoustic system may experience unintentional motion at 0.5 m/s (1 kt), which would account for $a = 3 \cdot 10^{-4}$. For an AUV moving at several m/s (submarines can move much faster), the factor a will be on the order of 10^{-3}, a value that cannot be ignored.

Nonnegligible motion-induced Doppler shifting and spreading thus emerge as another major factor that distinguishes an acoustic channel from the mobile radio channel, and dictates the need for explicit phase and delay synchronization in all but stationary systems [15.10]. In multicarrier systems, the Doppler effect creates a particularly severe distortion. Unlike in radio systems, where time compression/dilation is negligible and the Doppler shift appears equal for all frequencies within the signal bandwidth, in an acoustic system each frequency component may experience a markedly different Doppler shift, creating a nonuniform Doppler distortion across the signal bandwidth [15.44].

15.4.4 Time Variability: Random Effects (Fading)

Inherent channel changes range from the very large-scale, slow variations that occur seasonally (e.g., the change in sound speed profile from winter to summer) or daily (e.g., the change of water depth due to tides) to the small-scale, fast variations that are often caused by the rapid motion of the sea surface (waves) or the system itself. Many of these variations appear as random, and as such require an additional stage of modeling, namely statistical modeling.

The distinction between various scales is meaningful from the viewpoint of the duration of communication signals. While large-scale phenomena affect *average* signal power, causing it to vary over longer periods of time (many data packets), small-scale phenomena affect the *instantaneous* signal level, causing it to vary over shorter periods of time (few data packets, or bits of the same data packet). In light of system design, it is also useful to distinguish between those variations that are slow enough to admit a feedback by which the receiver can inform the transmitter of the change, and those that are too fast to be conveyed over the time it takes the signal to propagate from one end of the link to the other. In this sense, modeling of large-scale phenomena is meaningful for adaptive power control and modulation (which are performed at the transmitter in response to delayed feedback), while modeling of small-scale phenomena is important for adaptive signal processing at the receiver (channel estimation, equalization). It is also important to note that the apparently random channel variation can be a consequence of both the changes in the physical parameters of the environment (sound speed profile, surface scattering, internal waves) and the changes in the placement of the system within a given environment (transmitter/receiver displacement due to intentional motion or drifting with currents, etc.). Note also that these effects will differ across different environments, e.g., deep or shallow water, tropical, or ice-covered regions.

Large-Scale Effects

To assess the random variation of the channel, one can start by allowing the path lengths to deviate from the nominal values, so that

$$l_p = \bar{l}_p + \Delta l_p \,, \tag{15.14}$$

where Δl_p is regarded as a random displacement. This displacement models the large-scale variation which occurs because the channel geometry deviates from the nominal, either as the system is moved to a different location, or because the water depth has changed with the tide, etc. The deterministic, motion-induced delay variation which can be compensated through proper synchronization, is not considered as part of statistical channel analysis. The resulting transfer function of the channel, which is now *random* as well, is given by

$$H(f) = \overline{H}_0(f) \sum_p h_p e^{-i2\pi f \tau_p} \,, \tag{15.15}$$

where the path coefficients h_p can be calculated similarly as for the nominal case (15.7), using l_p instead of $\bar{l}_p$, and the delays can be calculated as $\tau_p = l_p/c - t_0$ in reference to some time $t_0 = \bar{l}_0/c$. The corresponding random path gains can also be approximated as [15.45]

$$h_p = \overline{h}_p e^{-\xi_p \Delta l_p/2} \,, \tag{15.16}$$

where

$$\xi_p = a_0 - 1 + k/\bar{l}_p \,, \tag{15.17}$$

and $\overline{h}_p$ is given by the expression (15.7). Note that one can also explicitly express the salient parameters h_p, τ_p as functions of time, i. e., $h_p(t), \tau_p(t)$, if one is interested in their variation during a long-term deployment in the *same* area (deep/shallow water, etc.).

Small-Scale Effects

The above model accounts only for the variations induced by the path length displacements, i. e., it does not include the effects of scattering. Scattering, which causes micro-path dispersion along each propagation path, can be modeled through an additional factor that accompanies the path gain $h_p(t)$. An overall channel model is now obtained in the form

$$H(f,t) = \overline{H}_0(f) \sum_p \gamma_p(f,t) h_p(t) e^{-i2\pi f \tau_p(t)} \,. \tag{15.18}$$

In this model, the factors $h_p(t)$ account for the slower-changing process caused by deviations of the system geometry from the nominal, while the factors $\gamma_p(f,t)$ represent the faster-changing scattering process. In other words, during a typical communication transaction of several packets, the path gains can be considered fixed, $h_p(t) = h_p$, but the additional factors $\gamma_p(f,t)$ cannot. Assuming a relatively large number of micro-paths, these factors can be modeled as complex-valued Gaussian processes, with some mean and variance. In general, scattering in an acoustic channel depends on the signal frequency, making each macro-path experience a different, possibly independent filtering effect. Note, however, that the transfer function $H(f,t)$ will in general exhibit correlation in both frequency and time (as well as across the elements of a transmit/receive array).

Statistical Characterization

Because of the different dynamics of the two types of processes, statistical channel analyses are typically conducted in two forms: one that targets the locally-averaged received signal power, and another that targets the instantaneous channel response. Specifically, large-scale statistical modeling focuses on the channel gain defined as

$$G(t) = \frac{1}{B} \int_{f_c - B/2}^{f_c + B/2} E_\gamma \left\{ \left| H^2(f,t) \right| \right\} \mathrm{d}f \,, \tag{15.19}$$

where the expectation is taken over small-scale fading. In contrast, small-scale modeling focuses on the processes $\gamma_p(f,t)$, as well as the effects of random Doppler shifting.

A complete statistical model for either large or small-scale phenomena must specify the probability density function (PDF) and the power spectral density (PSD), or the correlation properties of the random process of interest. These functions can be assessed using an analytical approach that relies on a mathematical model such as the one outlined above, a repeated application of a propagation model such as the Bellhop ray tracer for a large number of slightly disturbed channel conditions, or an experimental data analysis. All approaches have been considered in the literature, which abounds in statistical models that were found to adequately match the channels observed in different locations, at different time scales, and in different frequency bands. As of this time, however, the jury is still out on establishing standard models that would concisely describe the statistics of *typical* underwater acoustic channels. Crucial to that effort is identification of the scales of stationarity for the different processes at hand.

As far as the large-scale modeling goes, recent experimental results offer some evidence in support of a log-normal model for the channel gain [15.45–47]. Figure 15.12 illustrates such a model. Several of these studies also find that the path gains, and consequently the overall large-scale channel gain, can be well modeled as auto-regressive processes, at least on the time scales of several seconds, which are meaningful for implementation of packet-level feedback schemes.

Experimental studies on small-scale fading have offered evidence of Ricean [15.46, 48, 49] as well as Rayleigh phenomena [15.50]. Figure 15.13 illustrates an experimental data set that exhibits traits of Ricean fading. Combining the effects of large and small-scale fading leads to a mixture of log-normal and Ricean distributions, which can be approximated in closed form by the compound K-distribution. Experimental evidence to this effect is provided in [15.51]. Less is known about modeling the time-correlation functions of the small-scale processes, but it is generally understood that coherence times on the order of 100 ms can be assumed for a general-purpose design. Frequency-correlation, as well as space-correlation, as they pertain to communications systems, also remain to be addressed in a systematic manner.

The importance of statistical channel modeling is twofold. On the one hand, it enables the design of practical adaptive modulation methods which rely on identifying those channel parameters that can be *predicted* via delayed receiver-transmitter feedback [15.52]. On the other hand, it will enable the development standardized simulation models, thus allowing performance analy-

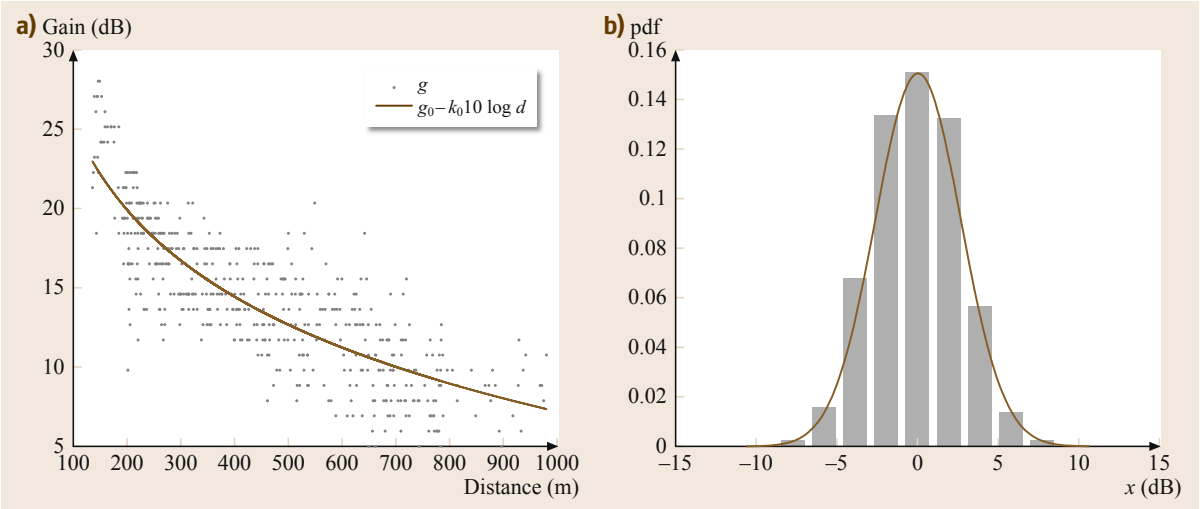

Fig. 15.12a,b During an experiment off the coast of Northern California, an acoustic signal occupying the 8–12 kHz band was transmitted between a fixed station and an AUV, and the strength of the signal received by the WHOI micro-modem was measured over a period of time during which the transmission distance changed. **(a)** shows the recorded signal strength, an estimate of the channel gain (15.19), as a function of distance (*dots*) and the accompanying trend which exhibits a log-distance dependence (*solid*). **(b)** shows the histogram of the difference between the recorded gain and the nominal trend, which is well described by a Gaussian distribution on the dB scale, i. e., a log-normal distribution on the linear scale

sis not only of signal processing methods, but also of network protocols and system-level design strategies, without the need for actual system deployment. Currently available simulators, such as the World Ocean Simulation System [15.53], use accurate ray tracing models, but they lack the statistical aspect of assessing the system performance. Statistical channel modeling was addressed recently in [15.45].

15.4.5 System Constraints

In addition to the fundamental limitations imposed by acoustic propagation, there are hardware constraints that affect the operation of acoustic modems. The most obvious of these constraints is the fact that acoustic transducers have their own bandwidth limitation, which constrains the available bandwidth beyond that offered by the channel. Additional constraints include power efficiency (transmitter amplifiers are often nonlinear, imposing a limit on the *peak* signal power), and the fact that acoustic modems operate in half-duplex fashion. These constraints do not only affect the physical link but all the layers of a network architecture. For example, the half-duplex mode of operation, combined with the low speed of sound, challenges the throughput efficiency of acoustic links that require automatic repeat request (ARQ) [15.54].

In an acoustic system, the power required for transmitting may be much greater than the power required for receiving. Transmission power depends on the distance, and its typical values are on the order of tens of Watts. (An acoustic signal propagates as a pressure wave, whose power is measured in Pascals, or commonly in dB relative to a micro Pascal. In seawater, 1 W of radiated acoustic power creates a sound field of intensity 172 dB re μPa 1 m away from the source.) In contrast, the power consumed by the receiver is much lower, with typical values ranging from about 100 mW for listening or low-complexity detection, to no more than a few Watts required to engage a sophisticated processor for high-rate signal detection. In hibernation mode, from which a modem can be woken on command, no more than 1 mW is required.

Underwater instruments are often battery-powered, and, hence, it is not simply the power, but the energy consumption that matters. This is less of an issue for mobile systems, where the power used for communication is a small fraction of the total power consumed for propulsion, but it is important for networks of fixed bottom-mounted nodes, where the overall network lifetime is the figure of merit. One way to save energy is by transmitting at a higher bit rate. For example, the WHOI modem [15.55] has two modes of operation: high rate at 5 kbps and low rate at 80 bps. This modem will require about 60 *times* less energy per bit (18 dB) in the high-rate mode. The receiver's energy consumption will also be lower, although it requires 3 W for detection of high-rate signals as opposed to 80 mW for detection of

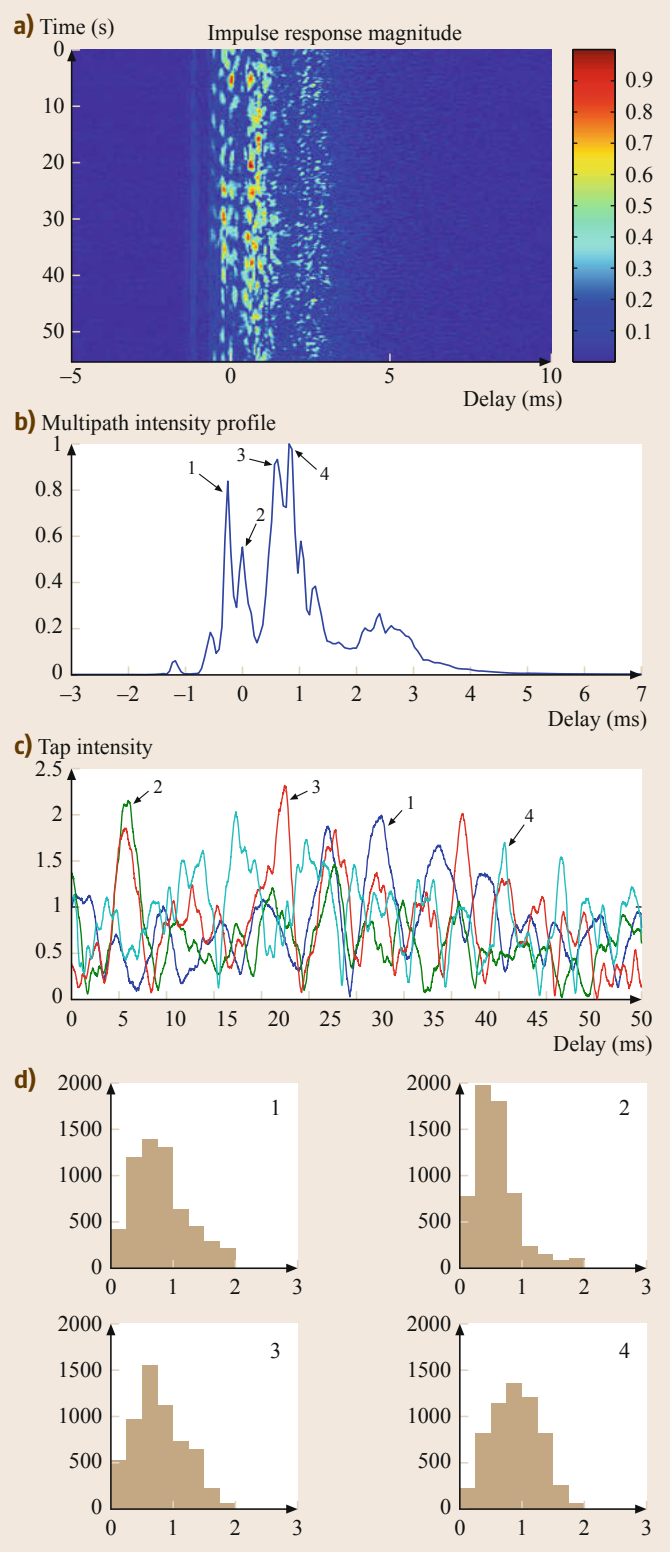

Fig. 15.13a–d During an experiment that took place in Narragansett Bay, near the coast of Rhode Island, the transmitter and the receiver were mounted on fixed tripods at 4 and 2 m above the bottom, at a distance of 1 km, with the channel depth ranging between 9 and 14 m. The sea condition was calm. A pseudo-random binary sequence of length 4095, modulated onto a 13 kHz carrier, was transmitted repeatedly at a rate of 10 kbps. The received signal was digitally down-converted, and correlated with the replica of the transmitted signal to yield an estimate of the channel response. Channel responses (magnitude) are shown in **(a)**. The multipath intensity profile **(b)** represents the average of magnitude-squared channel responses observed from 132 consecutive sequences. Shown also is the time-variation of several channel *taps* **(c,d)**. These figures reveal a channel consisting of multipath arrivals whose amplitude varies in time in a such a manner that there is no clearly defined strongest arrival. The phase (not shown) exhibits a random behavior around a constant slope, corresponding to a small but different Doppler shift on each of the arrivals, while the histograms of the tap magnitudes indicate Ricean fading

low-rate signals (the difference is about 2 dB). Another way to save the energy is by minimizing the number of retransmissions (we discuss the relevant protocols in Sect. 15.5.6). Finally, energy spent in idle listening over a longer period of time is not to be neglected. Having modems that are capable of hibernation, or instituting intentional sleeping schedules for those that are not, can help to control this type of power expenditure [15.56].

15.5 Point-to-Point Links: Signal Processing

15.5.1 Noncoherent Modulation/Detection

Noncoherent signaling is commonly used to relay data and to transmit command-and-control information at low bit rates. Frequency-hopped m-ary frequency-shift-key (FH-MFSK) modulation is widely accepted as a reliable albeit inefficient choice for such modems. FSK modulation uses distinct tonal or frequency-modulated pulses to map digital information. Frequency-hopping is a spread-spectrum technique, which alternates portions of the frequency band over fixed periods of time, so that successive FSK-modulated symbols use a different portion of the frequency spectrum, thus minimizing inter-symbol-interference (ISI) caused by reverberation. Many commercial suppliers offer several versions of FH-MFSK acoustic modems. In the case of a combination of N tones transmitted simultaneously, the symbol transmitted during the m-th signaling interval ($mT_s \le t < (m+1)T_s$) is

$$s_m(t) = A_m d(t) \sum_{n=1}^{N} g_{m,n} c_{m,n}(t), mT_s \le t < (m+1)T_s\,, \tag{15.20}$$

where, in the simplest case, $c_{m,n}(t)$ is a tone (either real or complex),

$$c_{m,n}(t) = e^{2\pi i f_{m,n}(t-mT_s)}, mT_s \le t < (m+1)T_s\,. \tag{15.21}$$

A_m is the peak acoustic pressure of symbol $s_m(t)$, $d(t)$ is the pulse shape (e.g., Gaussian), T_s is the pulse duration in seconds, $f_{m,n}$ is the carrier frequency of tone n for symbol $s_m(t)$. The binary information $b(m)$ is coded in symbol $s_m(t)$ as a combination $g_{m,n}$ of frequency bands centered at $f_{m,n} (n = 1, \ldots, N)$. $g_{m,n} = 1$ if the frequency band is used, otherwise $g_{m,n} = 0$ (at least one band is used for every symbol $s_m(t)$). If $s_m(t)$ uses only one of N bands and N is a power of 2, $\log_2(N)$ bits can be coded simultaneously within a single symbol. For example, if $N = 4$, $s_m(t)$ will contain $log_2(4) = 2$ bits of binary information ($b(m)$ =(0,0),(0,1),(1,0) or (1,1)). If $g_{1,n} = 1$ and $g_{2,n} = g_{3,n} = g_{4,n} = 0$, then $b_m = (0, 0)$. If $g_{2,n} = 1$ and $g_{1,n} = g_{3,n} = g_{4,n} = 0$, then $b_m = (0, 1)$, and so on. Figure 15.14 shows a section of an FH-MFSK modulated signal and the corresponding periodogram.

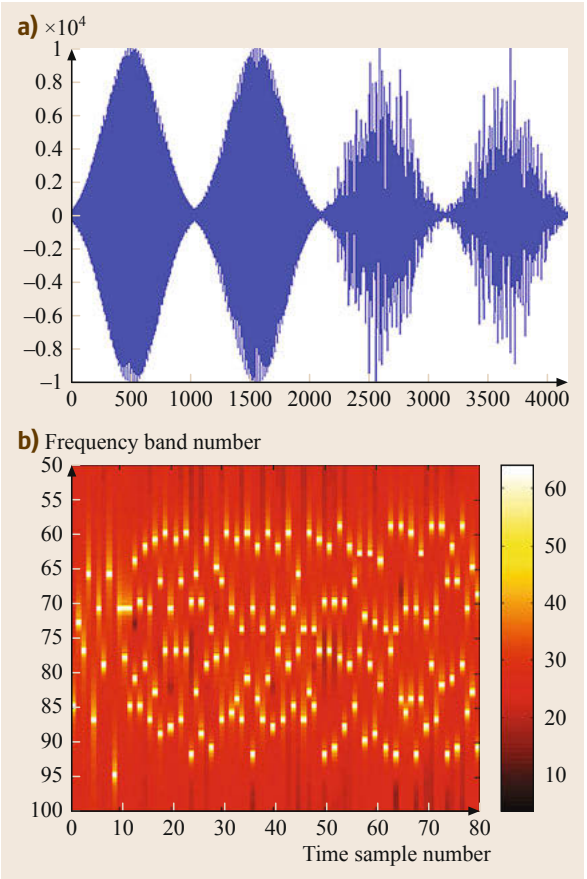

Fig. 15.14 (a) The first four symbols of a FH-MFSK sequence. (b) Spectrogram of a FH-MFSK sequence

At the receiver, the incoming message is first detected and synchronized using a short FH-MFSK modulated sequence. Following this, each data symbol is processed individually. First, the cross-correlation between the incoming faded symbol and a set of reference symbols $c_{m,n}(t)$ is computed,

$$R_{r_m,c_{m,n}}(\tau) = \int_{-T_s}^{T_s} r_m(t) c^*_{m,n}(t+\tau)\mathrm{d}t\,, \tag{15.22}$$

where * denotes the complex conjugate. For every received symbol $r_m(t)$, we retain the peak of correlation

within each band centered at $f_{m,n}$,

$$Z_{m,n} = \max_t \left\{ R_{r_m,c_{m,n}}(\tau); mT_s \le t < (m+1)T_s \right\} . \quad (15.23)$$

If we assume once more that $s_m(t)$ uses only one of N bands and N is a power of 2, we identify the frequency band that contains the most energy by comparing the coefficients $Z_{m,n}$,

$$n_{\max}(m) = \max_n \{Z_{m,n}; n = 1, \ldots, N\} . \quad (15.24)$$

Note that $n_{\max}$ is a function of the symbol index m. Under the same assumption, $g_{m,n} = 1$ if $n = n_{\max}$, otherwise $g_{m,n} = 0$. For example, if $n_{\max} = 1$, then $g_{m,1} = 1$ and $g_{m,2} = g_{m,3} = g_{m,4} = 0$. Therefore, $s_m(t)$ contains the couple of bits $b_m = (0, 0)$. If $n_{\max} = 2$, then $g_{m,2} = 1$ and $g_{m,1} = g_{m,3} = g_{m,4} = 0$, so that $s_m(t)$ contains the couple of bits $b_m = (0, 1)$, and so on.

15.5.2 Coherent Modulation/Detection

Coherent modulation methods include phase shift keying (PSK) and quadrature amplitude modulation (QAM). These methods offer bandwidth efficiency, i. e., the possibility to transmit more than 1 bit per second per Hertz of occupied bandwidth. However, because the information is encoded into the phase of the signal, precise knowledge of the received signal's frequency and phase is required in order to perform coherent detection. This fact presents a major challenge because an acoustic channel introduces a rather severe phase distortion on each of its multiple paths. A coherent receiver thus needs to perform phase synchronization together with channel equalization.

Coherent systems fall into two types: single-carrier and multicarrier systems. In single-carrier systems, a broadband information-bearing signal is directly modulated onto the carrier and transmitted over the channel. A typical high-rate acoustic signal occupies several kHz of bandwidth over which it experiences uneven channel distortion (Fig. 15.10). This distortion must be compensated at the receiver through the process of equalization. Multicarrier modulation bypasses this problem by converting the high-rate information stream into many parallel low-rate streams, which are then modulated onto separate carriers. The carriers are spaced closely enough such that the channel appears as frequency-flat in each narrow subband. After demodulation, each carrier's signal now only has to be weighted and phase-synchronized, i. e., a single-coefficient equalizer suffices per carrier. Each of these methods has its advantages and disadvantages when it comes to practical implementation: single-carrier systems are capable of faster channel tracking but they need high-maintenance equalizers; multicarrier systems are efficiently implemented using the fast Fourier transform (FFT), but they have high sensitivity to residual frequency offsets. In what follows, we review the basics of both types of systems as they apply to phase-distorted frequency-selective acoustic channels, and we outline the current research trends.

Single-Carrier Modulation/Detection

The problem of joint phase tracking and equalization in single-carrier broadband systems was addressed in [15.10]. The basic receiver structure [15.10] was extended to multichannel (array) configuration [15.57, 58] to enable diversity combining, which is often essential on acoustic channels. The resulting multichannel decision-feedback equalizer (DFE), integrated with a second-order phase-locked loop (PLL), provided the benchmark design for the high-speed acoustic modem [15.55]. It also became a de-facto standard for the development and comparison of future techniques, which focused on replacing the basic DFE with more sophisticated equalization and channel estimation schemes (e.g., turbo equalization and sparse channel estimation [15.39]), or inclusion of multiple transmitters, be it in the form of multiuser systems [15.59, 60] or multi-input multi-output (MIMO) structures for spatial multiplexing and/or diversity [15.38, 61].

The block diagram of a multichannel DFE is shown in Fig. 15.15. The receiver includes several stages: precombining (which may or may not be used, depending upon the array structure), phase correction, and multichannel equalization. The receiver is designed to process an incoming signal of the form

$$v(t) = \sum_n d(n) g_c(t - nT) e^{i\theta(t)} + w(t) , \quad (15.25)$$

where $d(n)$ are the data symbols transmitted at the rate of one symbol per T; $g_c(t) = g_T(t) * c(t) * g_R(t)$ is the composite impulse response of the transmitter, channel, and receiver (all in equivalent baseband with respect to the carrier frequency f_c); $\theta(t)$ is the carrier phase, and $w(t)$ is the noise. The channel response $c(t)$ and the phase $\theta(t)$ are unknown (and possibly different across the array elements), necessitating an adaptive receiver. Adaptive equalization has been considered in two forms: direct, which does not perform explicit channel estimation, and indirect, in which the channel is first estimated and then used to adjust the equalizer. In either form, the data symbols are estimated as

$$\hat{d}(n) = \sum_{p=1}^{P} \boldsymbol{a}_p^H(n) \boldsymbol{x}_p(n) e^{-i\hat{\theta}_p(n)} - \sum_{i>0} b_i^*(n) d(n-i) , \quad (15.26)$$

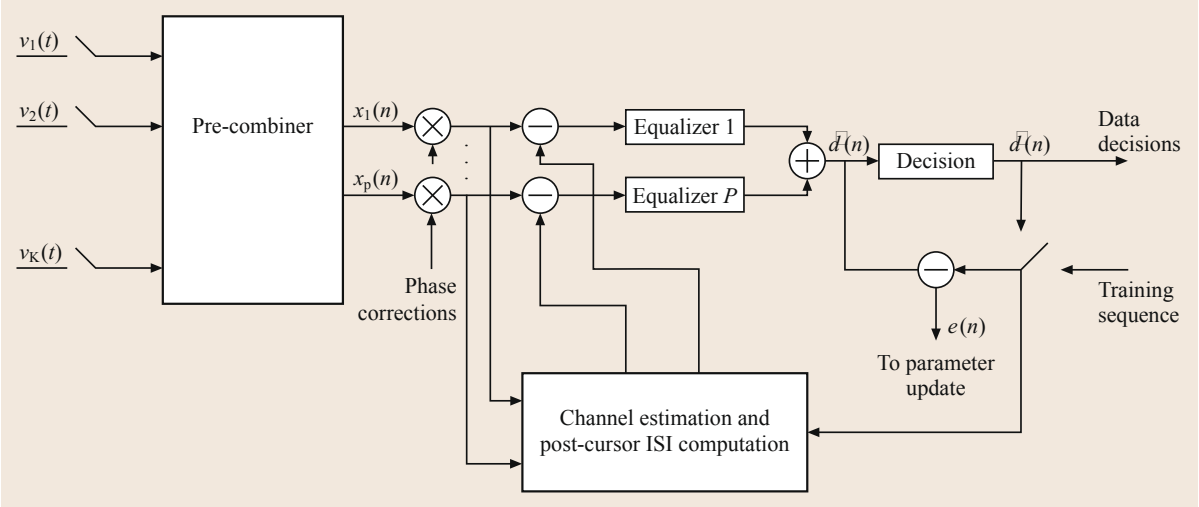

Fig. 15.15 Multichannel decision feedback equalizer

where the input vector $\boldsymbol{x}_p(n)$ to the p-th equalizer branch consists of the sampled precombiner output

$$x_p(t) = \sum_{k=1}^{K} c_{p,k}^{*} v^{(k)}(t) \, .$$

The samples are taken at the Nyquist rate, e.g., two per symbol interval for signals band-limited to $1/T$. The precombiner coefficients $c_{p,k}$, the feedforward equalizer vectors $\boldsymbol{a}_p$, the feedback equalizer coefficients b_i, and the phase estimates $\hat{\theta}_p$ are adjusted adaptively so as to minimize the mean squared error (MSE) in data detection. Each of these parameters is thus driven by the input signal and the error $e(n) = d(n) - \tilde{d}(n)$. Adaptive operation begins with a training sequence of known data symbols $d(n)$ until convergence has been established, after which the symbols $d(n)$ in (15.26) are replaced by the decisions $\tilde{d}(n)$ made on the estimates $\hat{d}(n)$. The details of various algorithm variants can be found in [15.36, 57, 58].

Performance of the multichannel DFE is illustrated in Fig. 15.16. The excellent performance achieved by this receiver in many environments testifies to the benefits of careful algorithm structuring that caters to the acoustic channel. While a propagation-ignorant design may result in an unnecessarily large number of receiver parameters (many equalizer branches with long filters), which will, in turn, cause increased sensitivity to noise and numerical errors, results similar to those of Fig. 15.16 show that one may not need more equalizer branches than there are significant propagation paths; that each of these branches may not need an excessively long filter, and that the feedback filter may only need to activate a select subset of coefficients, although its

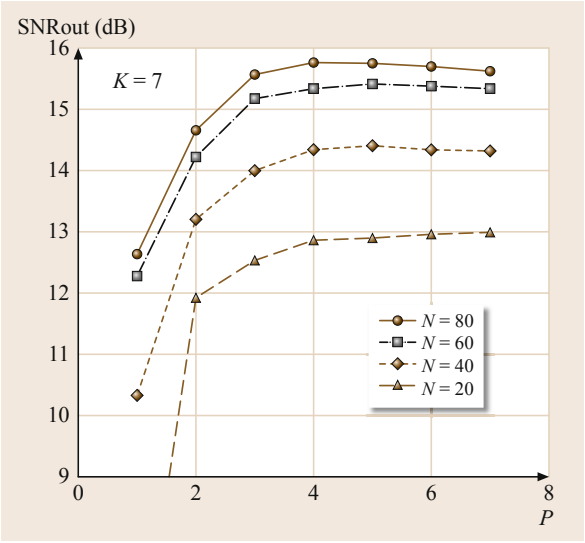

Fig. 15.16 Performance of the multichannel DFE on an experimental channel: output SNR (inversely proportional to the MSE) as a function of the number of equalizer channels P for a fixed number of input channels K. The parameter on the curves is the length N of each feedforward filter used. The total span of the feedback filter is 100 symbols. Real data used for this study correspond to quadrature amplitude modulation (QPSK) signals modulated at a rate of 2 kbps onto a carrier of 1 kHz, and transmitted acoustically over an 85 km long channel in about 50 m of water. The signals were received using a vertical array with interelement spacing of 1 m. The signals were processed using a double recursive least squares (RLS) algorithm integrated with a second-order decision-directed PLL ►

total span must match that of the multipath. In other words, respecting the *physical* aspects of acoustic propagation in developing a concise channel representation is the key to successful signal processing. Identification of *significant* channel components has attracted due interest in the acoustic community over the past several years, and much attention has been devoted to the topic of sparse channel estimation. [15.37] gives an excellent primer.

Multicarrier Modulation/Detection

Multicarrier modulation in the form of orthogonal frequency division multiplexing (OFDM) has been adopted as a standard for many of the emerging wireless radio systems – wireless local area networks (WLAN), digital audio and video broadcast (DAB/DVB), and long-term evolution that supports the fourth generation (4G) and future generations of cellular systems. However, it has only recently come into the forefront of acoustic communications research, and at the moment, there appears to be little effort to implement this technology in a commercial modem (e.g., by the French Thales).

The appeal of OFDM lies in the computational efficiency of FFT-based processing, and in the fact that it easily scales to different bandwidths (unlike with single-carrier systems, where the equalizer length has to be adjusted in accordance with the bandwidth B because it determines the symbol duration and hence the extent of ISI, with OFDM it simply suffices to increase/decrease the number of carriers K, i. e., the size of the FFT, while keeping the same carrier separation $\Delta f = B/K$). Namely, the demodulated signal is simply represented as

$$y_k(n) = H_k(n)d_k(n) + z_k(n)\,, \tag{15.27}$$

where $d_k(n)$ is the data symbol transmitted on the k-th carrier during the n-th OFDM block of duration $T = 1/\Delta f$; $H_k(n)$ is the channel transfer function $H(f,t)$ evaluated at the k-th carrier frequency at the time of the n-th block, and $z_k(n)$ is the noise. This signal admits a very simple detector, and extensions to multiple receiving elements are straightforward. In addition, by virtue of having a narrowband signal on each carrier, OFDM is easily conducive to MIMO processing [15.40, 62], adaptive modulation [15.63], and differentially coherent detection [15.64]. However, its sensitivity to frequency offset and time-variation of the channel demands special attention. Issues related to power efficiency also need to be kept in mind, as OFDM is sensitive to nonlinear distortions [15.65].

OFDM signal processing encompasses two stages: pre-FFT synchronization and post-FFT data detection. To account for motion-induced Doppler frequency shifting, which can amount to more than a full carrier spacing, front-end resampling is often necessary. A simple method for estimating the needed resampling rate is to measure the time between two synchronization preambles that frame several OFDM blocks and compare it to the expected frame duration [15.66].

Since the Doppler factor is relatively large to begin with (e.g., on the order of 10^{-3} for a relative velocity of 1.5 m/s), Doppler shifting that remains after initial resampling cannot be neglected. Two approaches have been pursued to address this issue: one is based on the assumption that residual Doppler shift is the same for all carriers [15.66], while another allows for nonuniform frequency shifting across the signal bandwidth [15.44].

Channel estimation for OFDM systems has been addressed in different forms: in one, each OFDM block is processed independently of the other blocks, thus allowing for the possibility that the channel changes completely from one block to another [15.41, 62], while another form exploits correlation between adjacent blocks [15.40, 67], which makes it advantageous on slowly varying channels. Similarly as in single-carrier systems, accurate channel estimation is the key to successful data detection in OFDM, and it benefits greatly from proper channel modeling to reduce the number of unknown parameters that need to be estimated. Methods for identification of sparse systems, such as matching pursuit (MP) and basis pursuit (BP), which improve upon traditional least squares (LS) estimation, were found to be beneficial and well suited to channel estimation in acoustic OFDM. These methods have been applied to both block-individual channel estimation that uses pilot carriers only [15.41], and to block-adaptive, decision-directed channel estimation [15.68].

The effect of time variability is a subtle one when it comes to acoustic OFDM systems: if the channel can change from one block to another, then perhaps it will change within each block. If this variation is nonnegligible, inter-carrier interference (ICI) will arise at the demodulator output, and carrier-by-carrier detection will no longer be optimal. ICI equalization then becomes necessary. Such a situation is somewhat counter-productive, as it destroys the original motivation of using OFDM for the simplicity of its implementation. Nonetheless, it may arise from pushing the limits of bandwidth efficiency: the more carriers in a given bandwidth, the better the bandwidth utilization, but the narrower the carrier spacing $\Delta f = 1/T$, the longer the OFDM block duration T, and the channel variation may become nonnegligible. The problem of ICI equalization is analogous to that of ISI equalization in single-carrier systems, except that the equalizer now operates across

carriers, and typically involves fewer interfering terms. Methods based on one-shot linear equalization of a full block of carriers [15.41, 69], as well as recursive linear or decision-feedback equalization [15.70], have been investigated. Further improvements are available from front-end (pre-FFT) filtering, which extracts the information about the time-varying channel before it has been lost in the process of FFT demodulation. A receiver that mimics the operation of an optimal, channel-matched filter was proposed in [15.71], while one that follows the analogy of fractionally-spaced equalization in the frequency domain was investigated in [15.72].

Virtually all acoustic OFDM systems addressed to date have focused on coherent detection and the attendant issues of channel estimation and Doppler tracking. However, a properly designed OFDM system (one in which there is no ICI) is well suited to differentially coherent detection as well. Differential encoding can be performed either across blocks or across carriers. In the latter case, differential coherence is naturally satisfied with tight carrier packing, which simultaneously supports bandwidth efficiency. Preliminary experimental results [15.64, 73] have demonstrated the benefits of differentially coherent OFDM, whose computational complexity is by far lower than that of any coherent system, and whose performance can surpass that of coherent detection when channel estimation fails.

15.5.3 Data Link Reliability

Channel coding or forward error coding (FEC) in a crucial feature of underwater acoustic modems. By introducing a redundancy part in the transmitted message, error correction codes allow for detection and correction of the bit errors caused by noise and inter-symbol interference. Generally, the ability to correct the errors is achieved by adding redundancy, which in turns reduces the effective data rate. Therefore, a proper coding scheme for a communication system is chosen based on the trade-off between the desired data bit rate and error rate performance.

Traditional FEC techniques are divided into convolutional codes (usually decoded with the ubiquitous Viterbi algorithm) and block codes (e.g., Bose-Chaudhuri-Hocquenghem or BCH, Reed–Solomon or RS) [15.74, 75]. Concatenated codes usually combine convolutional and block codes to improve the reliability of the acoustic modem even further. More recently, turbo codes [15.76, 77] and low-density parity-check (LDPC) codes [15.78] have become part of the field of telecommunication as they offer near Shannon error correction capability. Having inherently a low coding rate and a potentially large decoding latency, turbo codes have emerged as a good choice in communication systems where achieving a very low error rate performance is a top priority. A communication link designed for the transmission of the command-and-control messages to a remotely operated robot or vehicle is such a system. Since control messages do not contain a large number of bits that need to be transmitted in a short time, high bit rates are not required.

Even the most sophisticated error codes cannot ensure complete link reliability. To guarantee an error-free communication link (if it is physically possible), the acoustic modem must include a quality of service (QoS) feature, typically in the form of an automated retransmission query (ARQ) process implemented between two acoustic modems [15.54, 79]. This operation requires a communication protocol that includes acknowledgments and may dramatically reduce the overall data rate. The optimization of the QoS protocol is a key feature of modern acoustic modems. Acoustic modem users should be aware that commercially advertised throughputs (data rates) assume a single message transmission and do not include any retransmission.

15.5.4 Turbo Equalization

Turbo equalization is a very powerful method used to improve the removal of inter-symbol interference and additive noise. This technique can be implemented with single-carrier and multiple-carrier signaling. In particular, extensive research in combining turbo equalization and OFDM has taken place over the past decade. The simplest and best explanation is provided in the seminal work published in [15.80]. In short terms, turbo-equalization jointly optimizes adaptive equalization and channel decoding in an iterative process. The result is a dramatic improvement of transmission quality, even for high spectral efficiency modulations and time-varying fading channels. Modern underwater acoustic modems make growing use of this technique, which is powerful but processor intensive.

At the heart of this process is interleaving and error coding. The binary information at the source is carefully error-coded, modulated, and interleaved before it is pulse-shaped and transmitted through the water channel. In a traditional equalized receiver, the distorted signal is equalized, deinterleaved, converted to the binary domain, and the error-coded binary information is decoded and, hopefully, every binary error is corrected.

The obvious issue with this method is the fact that some error may remain. The turbo-equalizer goes two steps further in using this information. First of all, it modulates and interleaves the error-corrected binary information (which may still contain errors), thus cleaning the signal of some (or most of the) inter-symbol interference. The original signal is equalized

once again, but this time the *cleaned* signal is used as a new reference in the decision feedback portion of the adaptive equalizer. The second step is to repeat the entire operation again and again, so that the original signal is equalized against an ever *cleaner* reference signal.

The statistical properties of the acoustic channel, the type of interleaver, error coding, and decoding have a significant impact on turbo-equalizers. However, the same can be said of every equalized communication system, and overall this technique can lead to significant improvements in data transmission quality over a more traditional equalizer approach. Therefore, turbo-equalizers are becoming increasingly more common in underwater acoustic communication systems [15.38, 39, 69].

15.5.5 Adapting to the Environment

Adapting to the communication environment involves not only receiver-end channel estimation, but transmitter adaptation as well. This task is much more challenging in a time-varying environment which hinders the feedback from the receiver to the transmitter. In an acoustic channel, the situation is exacerbated by the long propagation delay which may make the feedback obsolete by the time it arrives. It is thus imperative to identify those environmental parameters that can withstand the feedback delay, and focus on the related transmitter functions.

In light of the large-scale and small-scale channel variations discussed in Sect. 15.4.4, adaptive mechanisms that have been considered include large-scale power control and small-scale waveform control. The first refers to adjusting the total transmitting power regardless of the modulation/detection method used, while the latter refers to adjusting the shape of the signal spectrum, i. e., distribution of the total available power over a given bandwidth. While the former targets power savings over extended periods of time (e.g., hours or days), the latter targets improved signal detection in a particular communication session (several data packets).

Neither type of adaptivity has been implemented in a commercial system, although research suggests significant benefits. Specifically, large-scale power control was shown to have significant benefits both in the sense of power savings [15.45] and in the sense of interference control in networked systems [15.81].

The work on small-scale adaptation has been versatile, including active time-reversal [15.82], single-mode excitation [15.83], and adaptive modulation [15.63]. Time reversal (or phase conjugation in the frequency domain) has in particular been extensively studied as an adaptive matched-filtering technique for acoustic communications [15.82], both in the sense of receiver adaptivity and transmitter adaptivity. It uses a time-reversed replica of a received signal waveform to implement a filter matched to that waveform, and can operate either passively or actively. Passive time-reversal resides at the receiver side only, where its role is to acquire a probe signal and use it to perform low-complexity front-end filtering prior to equalization or interference cancelation [15.84, 85]. In contrast, active time-reversal operates at the transmitter side, where its role is to time reverse the feedback signal and use it as the basic pulse (basic transmit waveform) that will best match the channel. By doing so, the transmitter, typically equipped with a large array, focuses its energy not only in time, but also in space ([15.82] and references therein). In repeated actions of this type, both ends of the link can focus their energy.

Adaptive modulation has been considered in the context of single-carrier MIMO systems [15.61], and, more recently, in the context of multicarrier systems [15.63], where adaptive power and/or rate control (adaptive bit loading) can be implemented easily by adjusting the amplitude and/or the modulation level of each carrier separately. The performance improvement available from these techniques is contingent on the quality of the channel state information that is fed back to the transmitter. Recent results [15.63], which report on the first experimental demonstration of this type, suggest the possibility to isolate the more slowly varying channel parameters (i. e., the predictable propagation path gains) from the more rapidly varying ones (phases) and use them to design an adaptive modulation system.

15.5.6 Networks

With the technological advances in acoustic modems, vehicles, and sensors, the concept of an underwater network of distributed autonomous nodes [15.14] is coming closer to realization. Experimental deployments are well underway, demonstrating the existing hardware capabilities in series of experimental deployments supported by the US Navy, such as the SeaWeb that uses telesonar modems [15.28], or deployments that use WHOI micro-modems [15.86]. Recently, efforts have begun to standardize acoustic network protocols with the goal of ensuring inter-operability between different modems. In particular, an international NATO-led effort is active in establishing JANUS [15.12], a standard that specifies data packet structures, acknowledgement (ACK) mechanisms, bit rates, etc., for use in given frequency band/transmissison distance configurations. Simultaneously, research is steadily advancing on the design of multiple-access methods, medium

access control (MAC) and routing protocols for underwater acoustic networks. The fundamental aspects of underwater acoustic networking have been highlighted in several survey articles [15.87–90]. At the moment, there is a solid base of custom-designed protocols that are suitable for poor-quality, interference-prone, delay-challenged acoustic channels, and are ready for testing in the field.

A full spectrum of network applications is not yet obvious, as integrated system capabilities depend on many aspects whose proof-of-concept, in turn, depends on in-situ testing. Unlike with signal processing, testing of networked systems cannot be performed off-line. Network simulation tools have thus started to emerge; an example is the World Ocean System Simulator (WOSS) [15.53], which integrates the Bellhop ray tracer with digital ocean maps and the NS-2 network simulator.

Due to a lack of *typical applications*, we tend to think about two types of networks: one with fixed, bottom-mounted nodes deployed for longer periods of time (e.g., sensor networks for environmental monitoring), and another with mobile nodes deployed on shorter missions (e.g., fleets of *cooperating* AUVs, where vehicles have the capability to respond to one another and make decisions, not only to be guided by supervisory commands from a central authority that amounts to *switch from mission A to mission B*). Interactions between mobile and fixed sensors are, of course, also of interest. Large-scale integration of autonomous systems includes the typical cross-layer network optimization at the boundary of two adjacent layers (i. e., routing and data link layer, or data link and physical layer). More importantly, it extends all the way from the application to the physical link, and includes external system functions such as localization and navigation (which themselves are challenging tasks as there is no global positioning or timing underwater).

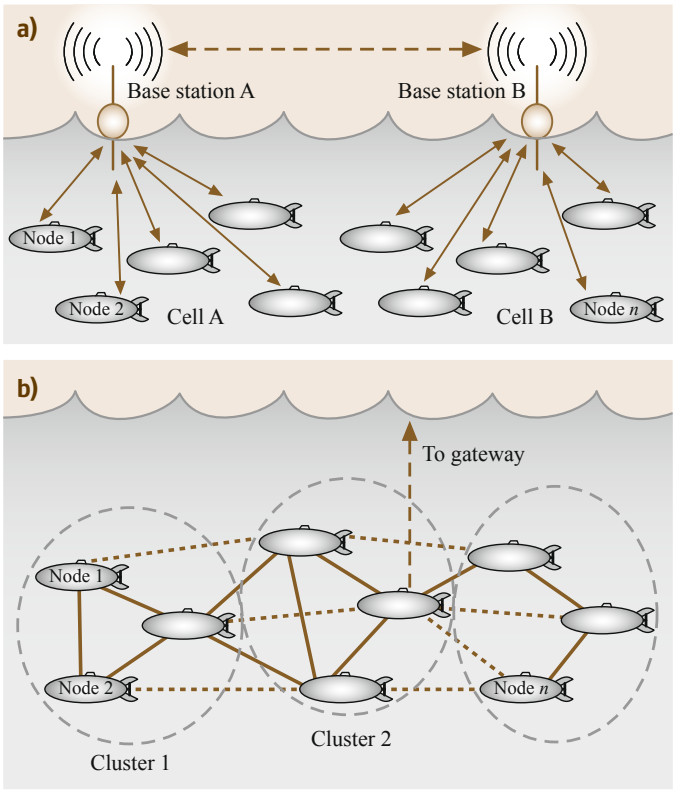

Fig. 15.17a,b Network topologies and the associated architectures come in various forms: in a centralized network of a cellular type, nodes communicate through a single-hop connection to the base station, while base stations are connected to a common infrastructure **(a)**; in a de-centralized network of an ad-hoc type, nodes communicate over multihop, peer-to-peer links **(b)**

The design of underwater networks is daunted by the constraints of acoustic propagation: limited, distance-dependent bandwidth, high bit (packet) error rate, and high channel latency. The fact that acoustic signals propagate at 1500 m/s, while bit rates supported by the (half-duplex) acoustic modems are on the order of a kbit/s, makes the propagation delay anything but negligible with respect to the packet size – otherwise a common assumption in the design of many channel access schemes. As a result, direct application of protocols developed for terrestrial sensor networks may incur a serious penalty in efficiency, requiring instead a careful re-design for acoustic applications. Energy efficiency is an important aspect in bottom-mounted sensor networks, since recharging the batteries of submerged instruments is to be postponed for as long as possible. In contrast, mobile systems are already constrained to several-hour missions before they have to re-charge, and power usage for communications is not a major issue (unless self-propelled gliders are in question). It must also be kept in mind that underwater instruments (sensors, modems, vehicles) are neither cheap nor disposable. This fact may be the single most-important feature that distinguishes underwater networks from their terrestrial counterparts, fundamentally changing many network design principles that are usually taken for granted. Finally, the questions of network topology optimization and the associated capacity analysis remain open.

In terms of system topology and architecture, two extreme situations are illustrated in Fig. 15.17. In a centralized network, distributed nodes communicate through a base station in whose footprint they are. Coverage can be extended in this type of network by replicating the cells across space, similarly as in terrestrial cellular systems (except that the *infrastructure* that connects the base stations can consist of radio links). In a de-centralized network, the nodes communicate di-

rectly with each other. There is no central authority such as a base station, although the nodes can form clusters, and the end goal may as well be to transmit all the data to a common node (a surface sink). The network nodes can either have pre-established routes over which to send the packets (as would be the case in fixed bottom-mounted networks), or they can do this in an ad-hoc manner, learning the routes as they go (which would be the case in a mobile network). Between these two extremes lie various hybrid architectures.

15.5.7 Channel Sharing

Channel sharing is the major design issue for band-limited acoustic networks. Methods for channel sharing can be divided into two types: deterministic and random. In deterministic access, resources such as frequency bands or time slots are allocated to particular nodes. This type of multiple access is well suited to systems in which the nodes transmit continuously, since the a-priori allocated resources are then well utilized. If the nodes instead transmit in a bursty manner and not too often, random access may be the preferred choice. The nodes now transmit more-or-less at their own will and in the same frequency band, risking a loss if their packets collide at the receiver. Medium access control (MAC) protocols can then be used to orchestrate the nodes' behavior and reduce the chances of collision. Random and deterministic access can also be combined in a reservation-based channel sharing scheme. Nodes now first contend by transmitting short reservation packets in a random access fashion. The central authority chooses the winners, and deterministically allocates them fixed resources for the duration of the data transmission phase.

Deterministic Access

Deterministic access for acoustic networks has been considered in various forms – frequency, time, and code-division multiple access (FDMA, TDMA, CDMA) [15.91]. Typically, FDMA is considered inefficient on account of the fact that the already limited bandwidth will be wasted if allocated permanently to a node that does not transmit, while those nodes that transmit will be doing so at a lower bit rate, thereby increasing the energy consumption. This reasoning is justified in today's applications where the nodes typically do not stream continuously, but only report to the base station upon request. A polling mechanism is then put in place via time-division duplexing (TDD). Although this method may resemble TDMA (and is often called that) a network based on polling is not a true TDMA network, as it involves a two-way propagation delay for each transaction, whereas in a true TDMA network nodes schedule their transmissions so that they arrive back-to-back to the central node. In an acoustic setting with variable propagation delays, guard times are needed to ensure that there is no overlap of packets at the base station. Acoustic modems that are currently in use are well conducive to such an implementation [15.92].

An alternative that has been considered for small multiuser systems is CDMA based on direct-sequence spread-spectrum (DS-SS) modulation, which simultaneously provides the low probability of detection (LPD) needed for operation in hostile environments. It may be worth noting that the usual assumptions involved in the design of radio DS-SS systems do not hold in an acoustic channel, because it requires chip-rate (as opposed to symbol-rate) adaptive processing to take advantage of the available spreading gain [15.60]. Passive time reversal has also been used for multiuser detection [15.85].

While today's applications do not require more than a single cell, spatial frequency reuse across multiple cells offers the key to large area coverage with a limited bandwidth. Acoustic propagation, however, dictates cellular design principles that are more complex than those used in terrestrial networks, and makes the system capacity heavily dependent on the center frequency [15.93]. Specifically, moving to a higher frequency region than that dictated by simple SNR maximization (Fig. 15.5) improves the signal-to-interference ratio and yields a greater capacity.

Random Access

Random access has been used for acoustic networks in which the nodes transmit infrequently [15.28, 86]. This type of access is also suitable for networks with many nodes, so long as the their aggregate traffic does not exceed a certain limit. The simplest form of random access is the Aloha mechanism whereby each node transmits whenever it wants to, and if it becomes aware of a collision (via an acknowledgement/negative acknowledgement (ACK/NAK) feedback from the intended receiver), it re-transmits after a random back-off time. This simple mechanism can be augmented by carrier sensing multiple access (CSMA), which imposes an additional condition that a node can transmit only if it senses the channel to be free. Compared to radio systems where propagation delay is negligible compared to the packet duration, this listen-before-transmitting principle has fewer benefits in acoustic systems, where the packets propagate slowly, and the fact that none are overheard does not mean that some are not present in the channel. Multiple-access collision avoidance (MACA) introduces a hand-shaking procedure to secure the link using short control packets of

the request-to-send/clear-to-send type (RTS/CTS) prior to transmitting the longer data packets.

In the past years there have been major developments on the medium access control (MAC) layer, with focus on protocol design that is not ignorant of the high acoustic latency, but strives to overcome it in an efficient manner or even take advantage of it. Examples of such protocols include the distance-aware collision avoidance protocol (DACAP) [15.94], T-Lohi [15.95], propagation-delay-tolerant Aloha [15.96], and many others, e.g., [15.97, 98]. For example, DACAP is based on a standard control packet exchange to secure the link for data transmission, with the addition of a warning signal that interrupts an on-going transmission that is bound to fail. T-Lohi uses dedicated collision-avoidance tones to announce data transmission, thus enabling all those who overhear the tones to count the number of active nodes, which, in turn, is used to optimize channel access.

15.5.8 Routing and Cross-Layer Integration

Work on higher layer protocols has focused in particular on routing. Geographical routing, which exploits the knowledge of the nodes' locations to determine the best next relay so as to minimize the total energy consumption, was addressed in [15.99]. A distributed geographical routing protocol with integrated power control was proposed in [15.81]. Distributed routing for delay-sensitive and delay-insensitive applications was investigated in [15.100], while a distributed procedure for initial neighbor discovery was proposed in [15.101]. Transport control protocols have been considered to a much lesser extent, since end-to-end retransmission suffers greatly from long delays and high packet error rate.

Cross-layer design plays an important role in acoustic systems, both between adjacent network layers and between adjacent system functions. Examples of cross-layer design include frequency allocation and power control integration with MAC and routing [15.81]; topology/sleep control for energy-efficiency in fixed networks [15.56, 98, 102]; packet size selection for optimizing the throughput/energy performance of MAC protocols [15.103], and optimization of rateless packet coding (network coding) for use with half-duplex acoustic links [15.104]. An example of cross-*function* design is integration of localization/navigation with acoustic communications. The use of acoustic modems as traveling beacons that help to localize AUVs by measuring the relative propagation delays in a network is described in [15.92]. Such localization may, in turn, support geographical routing protocols in which location information is used to find the best routes through the network.

The issues of mobility and delay-tolerance have received particular attention. Channel access in a network composed of both fixed and mobile nodes was studied in [15.102], via a simulation analysis that compares the Aloha and the DACAP protocols. Both were found to provide satisfactory performance, which is further enhanced for mobile applications by simple modifications such as back-to-back repetitions. [15.105] investigated routing in a delay-tolerant network (DTN), comparing two classes of protocols, one based on spray-and-wait principle and the other based on resource allocation for intentional DTN. In conditions of high load, the latter was found to outperform the former as well as basic flooding in terms of packet delivery ratio regardless of mobility conditions, while the former showed better performance in terms of average delivery ratio. [15.106] considered a swarm of free-floating mobile sensor nodes that need to report their measurements to a central station. [15.107] considered location-based routing in a mobile network. To improve the performance, the nodes do not use the current knowledge of the destination's location, but instead form a prediction based on the history of motion. [15.108] also investigated location-based routing, which it enhanced by inclusion of a link quality metric into the decision-making process. Finally, [15.109] explored the idea of waiting for a favorable link to present itself before forwarding a packet. In other words, an AUV may not wish to waste its energy transmitting to a relay far away, but may instead want to wait for a better opportunity. Once such an opportunity presents itself, highly directional transmission is exploited to focus the energy in a desired direction.

These references offer a valuable first step towards understanding the network behavior in the presence of long acoustic delay and frequency-dependent attenuation. They identify vulnerable points of existing protocols and offer clever solutions to recover the performance. However, although there is a common understanding that mobility needs special care in an acoustic setting, the analysis is often conducted via simulation, using a time-invariant propagation model. This fact emphasizes the need for *statistical* channel models that will reflect temporal as well as spatial variability of acoustic channel and enable the development of more accurate simulation tools.

15.6 Future Trends

As underwater acoustic modem technology keeps evolving, new research trends appear. The most obvious trend is the development of message format and protocols optimized for a specific application. A good example is the development of the compact control language (CCL) for unmanned underwater vehicle (UUV) applications [15.23]. Another example is digital diver modems. In addition, data compression algorithms tailored for underwater acoustic modems have now been developed, as traditional compression routines are often not well suited to this type of communication system. The integration of underwater acoustic modems in larger system now includes the combination of multiple functions in order to reduce cost, size, and power consumption. For example, several underwater acoustic modems also include long-baseline and/or ultra-short baseline acoustic positioning capability [15.110, 111].

Some of the most innovative research in underwater communication now combines various modalities, such as optics (laser, lidar), and magnetic and electromagnetic signaling with broadband acoustics [15.112]. In particular, excellent work is taking place in combining short-range, high-bit-rate underwater communications with slower, longer-range underwater acoustic communications. Finally, one should not overlook the extensive research work taking place to develop better acoustic propagation models and statistical performance models [15.113]. For example, great efforts are being made in modeling and optimizing network operations using underwater acoustic modems, possibly in combination with surface radio communication devices. Also, integrated underwater acoustic communications and localization are increasingly being combined to improve data routing [15.114].

References

15.1 X. Che, I. Wells, G. Dickers, P. Kear, X. Gong: Re-evaluation of RF electromagnetic communication in underwater sensor networks, IEEE Commun. Mag. **48**(12), 143–151 (2010)

15.2 N. Farr, A. Bowen, J. Ware, C. Pontbriand, M. Tivey: An integrated, underwater optical /acoustic communications system, Proc. IEEE OCEANS'10 (2010) pp. 1–6

15.3 L. Freitag, S. Singh: Performance of micro-modem PSK signaling under variable conditions during the 2008 RACE and SPACE experiments, Proc. MTS/IEEE OCEANS'09 (2009) pp. 1–8

15.4 L. Freitag, M. Stojanovic: Basin-scale acoustic communication: a feasibility study using tomography m-sequences, Proc. MTS/IEEE OCEANS'01, Vol. 4 (2001) pp. 2256–2261

15.5 L. Freitag, M. Johnson, D. Frye: High-rate acoustic communications for ocean observatories-performance testing over a 3000 vertical path, Proc. MTS/IEEE OCEANS'00, Vol. 2 (2000) pp. 1443–1448

15.6 A. Quazi, W. Konrad: Underwater acoustic communications, IEEE Commun. Mag. **20**(2), 24–30 (1982)

15.7 A.B. Baggeroer, D.E. Koelsch, K. von der Heydt, J. Catipovic: DATS - A digital acoustic telemetry system for underwater communications, Proc. IEEE OCEANS'81 (1981) pp. 55–60

15.8 J. Catipovic, D. Brady, S. Etchemendy: Development of underwater acoustic modems and networks, Oceanography **6**(3), 112–119 (1993)

15.9 M.D. Green, J.A. Rice: Channel-tolerant FH-MFSK acoustic signaling for undersea communications and networks, IEEE-JOE **25**(1), 28–39 (2000)

15.10 M. Stojanovic, J.A. Catipovic, J.G. Proakis: Phase-coherent digital communications for underwater acoustic channels, IEEE-JOE **19**(1), 100–111 (1994)

15.11 S. Singh, S.E. Webster, L. Freitag, L.L. Whitcomb, K. Ball, J. Bailey, C. Taylor: Acoustic communication performance of the WHOI micro-modem in sea trials of the Nereus vehicle to 11,000 m depth, Proc. IEEE OCEANS'09 (2009) pp. 1–6

15.12 J.R. Potter, A. Berni, J. Alves, D. Merani, G. Zappa, R. Been: Underwater communications protocols and architecture developments at NURC, Proc. IEEE OCEANS'11 (2011) pp. 1–6

15.13 V. Tunnicliffe, C.R. Barnes, R. Dewey: Major advances in cabled ocean observatories (VENUS and NEPTUNE Canada) in coastal and deep sea settings, Proc. IEEE/OES US/EU-Balt. Int. Symp. (2008) pp. 1–7

15.14 T.B. Curtin, J.G. Bellingham, J. Catipovic, D. Webb: Autonomous oceanographic sampling networks, Oceanography **6**(3), 86–94 (1993)

15.15 Teledyne Benthos: https://teledynebenthos.com/product/acoustic_modems/910-series-atm-916

15.16 Woods Hole Oceanographic Institution: http://acomms.whoi.edu/micro-modem

15.17 LinkQuest Inc.: http://www.link-quest.com/html/uwm1000.htm

15.18 EvoLogics: http://www.evologics.de/en/products/acoustics/index.html

15.19 Sercel: http://www.sercel.com/products/Pages/mats3g.aspx

15.20 L-3 Oceania: http://www2.l-3com.com/oceania/products/uc_modem.htm

15.21 Tritech: http://www.tritech.co.uk/product/micron-data-modem

15.22 P.-P.J. Beaujean, E. Carlson: HERMES – A high bit-rate underwater acoustic modem operating at high-frequencies for ports and shallow wa-

ter applications, Mar. Technol. Soc. J. **43**(2), 21–32 (2009)
15.23 R.P. Stokey, L.E. Freitag, M.D. Grund: A compact control language for AUV acoustic communication, Proc. IEEE OCEANS'05 (2005) pp. 1133–1137
15.24 D.B. Kilfoyle, A.B. Baggeroer: The state of the art in underwater acoustic telemetry, IEEE-JOE **25**(1), 4–27 (2000)
15.25 R.J. Urick: *Principles of Underwater Sound*, 3rd edn. (McGraw-Hill, New York 1983)
15.26 H. Medwin, C.S. Clay: *Fundamentals of Acoustical Oceanography (Applications of Modern Acoustics)* (Academic Press, Waltham 1998)
15.27 M.B. Porter, V.K. McDonald, P.A. Baxley, J.A. Rice: SignalEx: Linking environmental acoustics with the signaling schemes, Proc. MTS/IEEE OCEANS'00 (2000) pp. 595–600
15.28 J.A. Rice, C.W. Ong: A discovery process for initializing underwater acoustic networks, Proc. SENSORCOMM (2010) pp. 408–415
15.29 L. Berkhovskikh, Y. Lysanov: *Fundamentals of Ocean Acoustics*, Springer Series in Electronics and Photonics, Vol. 8 (Springer, Berlin, Heidelberg 1982)
15.30 M. Stojanovic: On the relationship between capacity and distance in an underwater acoustic communication channel, Proc. WUWNet (2006) pp. 41–47
15.31 M. Stojanovic: Capacity of a relay acoustic channel, Proc. IEEE OCEANS'07 (2007) pp. 1–7
15.32 M.Porter: Ocean Acoustics Library, http://oalib.hlsresearch.com/ (2015)
15.33 M.B. Porter, H.P. Bucker: Gaussian beam tracing for computing ocean acoustic fields, J. Acoust. Soc. Am. **82**(4), 1349–1359 (1987)
15.34 M. Siderius, M.B. Porter: Modeling broadband ocean acoustic transmissions with time-varying sea surfaces, J. Acoust. Soc. Am. **124**, 137–150 (2008)
15.35 F.F. Jensen, W. Kuperman, M. Porter, H. Schmidt: *Computational Ocean Acoustics*, Modern Acoustics and Signal Processing (Springer, New York 2011)
15.36 M. Stojanovic: Efficient processing of acoustic signals for high rate information transmission over sparse underwater channels, Phys. Commun. **1**(2), 146–161 (2008)
15.37 W. Li, J.C. Preisig: Estimation of rapidly time-varying sparse channels, IEEE-JOE **32**(4), 927–939 (2007)
15.38 S. Roy, T.M. Duman, V.K. McDonald: Error rate improvement in underwater MIMO communications using sparse partial response equalization, IEEE-JOE **34**(2), 181–201 (2009)
15.39 J.W. Choi, T.J. Riedl, K. Kim, A.C. Singer, J.C. Preisig: Adaptive linear turbo equalization over doubly selective channels, IEEE-JOE **36**(4), 473–489 (2011)
15.40 M. Stojanovic: MIMO OFDM over underwater acoustic channels, Proc. 43rd Asilomar Conf. Signals Syst. Comput. (2009) pp. 605–609
15.41 C.R. Berger, S. Zhou, J.C. Preisig, P. Willett: Sparse channel estimation for multicarrier underwater acoustic communication: From subspace methods to compressed sensing, IEEE Trans. Sig. Process. **58**(3), 1708–1721 (2010)
15.42 T. Kang, R.A. Iltis: Iterative carrier frequency offset and channel estimation for underwater acoustic OFDM systems, IEEE J. Sel. Areas Commun. **26**(9), 1650–1661 (2008)
15.43 M.M. Stojanovic, J. Catipovic, J. Proakis: Performance of High-Rate Adaptive Equalization on a Shallow Water Acoustic Channel, J. Acoust. Soc. Am. (1996) pp. 2213–2219
15.44 M. Stojanovic: Low complexity OFDM detector for underwater acoustic channels, Proc. IEEE OCEANS'06 (2006) pp. 1–6
15.45 P. Qarabaqi, M. Stojanovic: Statistical characterization and computationally efficient modeling of a class of underwater acoustic communication channels, IEEE-JOE **38**(4), 701–717 (2013)
15.46 W.B. Yang, T.C. Yang: High-frequency channel characterization for M-ary frequency-shift-keying underwater acoustic communications, J. Acoust. Soc. Am. **120**(5), 2615–2626 (2006)
15.47 B. Tomasi, G. Zappa, K. McCoy, P. Casari, M. Zorzi: Experimental study of the space-time properties of acoustic channels for underwater communications, Proc. IEEE OCEANS'10 (2010) pp. 1–9
15.48 A. Radosevic, D. Fertonani, T.M. Duman, J.G. Proakis, M. Stojanovic: Capacity of MIMO systems in shallow water acoustic channels, Proc. 44th Asilomar Conf. Sig. Syst. Comput. (2010) pp. 2164–2168
15.49 F. Socheleau, C. Laot, J. Passerieux: Stochastic replay of non-WSSUS underwater acoustic communication channels recorded at sea, IEEE Trans. Signal Process. **59**(10), 4838–4849 (2011)
15.50 M. Chitre: A high-frequency warm shallow water acoustic communications channel model and measurements, J. Acoust. Soc. Am. **122**(5), 2580–2586 (2007)
15.51 J. Zhang, J. Cross, Y.R. Zheng: Statistical channel modeling of wireless shallow water acoustic communications from experiment data, Proc. MILCOM (2010) pp. 2412–2416
15.52 A. Radosevic, T.M. Duman, J.G. Proakis, M. Stojanovic: Channel prediction for adaptive modulation in underwater acoustic communications, Proc. IEEE OCEANS'11 (2011) pp. 1–5
15.53 F. Guerra, P. Casari, A. Berni, J. Potter, M. Zorzi: Performance evaluation of random and handshake-based channel access in collaborative mobile underwater networks, Proc. OCEANS'10 (2010) pp. 1–7
15.54 M. Stojanovic: Optimization of a data link protocol for an underwater acoustic channel, Proc. IEEE OCEANS'05, Vol. 1 (2005) pp. 68–73
15.55 L. Freitag, M. Grund, S. Singh, J. Partan, P. Koski, K. Ball: The WHOI micro-modem: An acoustic communications and navigation system for multiple platforms, Proc. MTS/IEEE OCEANS'05, Vol. 2 (2005) pp. 1086–1092

15.56 A. Harris, M. Stojanovic, M. Zorzi: Idle-time energy savings through wake-up modes in underwater acoustic networks, Elsevier J. Ad Hoc Netw. **7**, 770–777 (2009)

15.57 M.M. Stojanovic, J. Catipovic, J. Proakis: Adaptive multichannel combining and equalization for underwater acoustic communications, J. Acoust. Soc. Am. (1993) pp. 1621–1631

15.58 M. Stojanovic, J.G. Proakis, J. Catipovic: Reduced complexity spatial and temporal processing of underwater acoustic communication signals, J. Acoust. Soc. Am. **98**(2), 961–972 (1995)

15.59 M. Stojanovic, Z. Zvonar: Multichannel processing of broad-band multiuser communication signals in shallow water acoustic channels, IEEE-JOE **21**(2), 156–166 (1996)

15.60 M. Stojanovic, L. Freitag: Multichannel detection for wideband underwater acoustic CDMA communications, IEEE-JOE **31**(3), 685–695 (2006)

15.61 D.B. Kilfoyle, J.C. Preisig, A.B. Baggeroer: Spatial modulation experiments in the underwater acoustic channel, IEEE-JOE **30**(2), 406–415 (2005)

15.62 B. Li, J. Huang, S. Zhou, K. Ball, M. Stojanovic, L. Freitag, P. Willett: MIMO-OFDM for high-rate underwater acoustic communications, IEEE-JOE **34**(4), 634–644 (2009)

15.63 A. Radosevic, R. Ahmed, T.M. Duman, J.G. Proakis, M. Stojanovic: Adaptive OFDM modulation for underwater acoustic communications: Design considerations and experimental results, IEEE-JOE **39**(2), 1–14 (2013)

15.64 Y. Aval, M. Stojanovic: A method for differentially coherent multichannel processing of acoustic OFDM signals, Proc. IEEE Workshop Sensor Array Multichannel Signal Process. (SAM) (2012)

15.65 G. Rojo, M. Stojanovic: Peak-to-average power ratio (PAR) reduction for acoustic OFDM systems, MTS J. **44**(4), 30–41 (2010)

15.66 B. Li, S. Zhou, M. Stojanovic, L. Freitag, P. Willett: Multicarrier communication over underwater acoustic channels with nonuniform doppler shifts, IEEE-JOE **33**(2), 198–209 (2008)

15.67 P. Ceballos Carrascosa, M. Stojanovic: Adaptive channel estimation and data detection for underwater acoustic MIMO OFDM systems, IEEE-JOE **35**(3), 635–646 (2010)

15.68 A. Radosevic, T.M. Duman, J.G. Proakis, M. Stojanovic: Selective decision directed channel estimation for UWA OFDM systems, Proc. 49th Commun. Control Comput. (2011) pp. 647–653

15.69 J. Huang, S. Zhou, J. Huang, C.R. Berger, P. Willett: Progressive inter-carrier interference equalization for OFDM transmission over time-varying underwater acoustic channels, IEEE J. Sel. Top. Signal Process. **5**(8), 1524–1536 (2011)

15.70 K. Tu, D. Fertonani, T.M. Duman, M. Stojanovic, J.G. Proakis, P. Hursky: Mitigation of intercarrier interference for OFDM over time-varying underwater acoustic channels, IEEE-JOE **36**(2), 156–171 (2011)

15.71 S. Yerramalli, M. Stojanovic, U. Mitra: Partial FFT demodulation: A detection method for highly doppler distorted OFDM systems, IEEE Trans. Signal Process. **60**(11), 5906–5918 (2012)

15.72 Z. Wang, S. Zhou, G.B. Giannakis, C.R. Berger, J. Huang: Frequency-domain oversampling for zero-padded OFDM in underwater acoustic communications, IEEE-JOE **37**(1), 14–24 (2012)

15.73 Y.M. Aval, M. Stojanovic: Fractional FFT demodulation for differentially coherent detection of acoustic OFDM signals, Proc. 46th Conf. Signals Syst. Comput. (ASILOMAR) (2012) pp. 1525–1529

15.74 S. Lin, D.J. Costello: *Error Control Coding: Fundamentals and Applications* (Prentice Hall, Englewood Cliffs 1983)

15.75 B. Sklar: *Digital Communications* (Prentice Hall, Englewood Cliffs 1988)

15.76 C. Berrou, A. Glavieux: Near optimum error correcting coding and decoding: turbo-codes, IEEE Trans. Commun. **44**(10), 1261–1271 (1996)

15.77 M. Pajovic, P.-P. Beaujean: Turbo-coded frequency-hopped frequency division multiplexed signaling for underwater acoustic communications between 60 and 90 kHz in ports and very shallow waters, Proc. MTS/IEEE OCEANS'09 (2009) pp. 1–7

15.78 J. Huang, S. Zhou, P. Willett: Nonbinary LDPC coding for multicarrier underwater acoustic communication, IEEE J. Sel. Areas Commun. **26**(9), 1684–1696 (2008)

15.79 B. Tomasi, P. Casari, L. Badia, M. Zorzi: A study of incremental redundancy hybrid ARQ over Markov channel models derived from experimental data, Proc. WUWNet (2010)

15.80 C. Laot, A. Glavieux, J. Labat: Turbo equalization: Adaptive equalization and channel decoding jointly optimized, IEEE J. Sel. Areas Commun. **19**(9), 1744–1751 (2001)

15.81 J. Montana, M. Stojanovic, M. Zorzi: On joint frequency and power allocation in a cross-layer protocol for underwater acoustic networks, IEEE-JOE **35**(4), 936–947 (2010)

15.82 G.F. Edelmann, H.C. Song, S. Kim, W.S. Hodgkiss, W.A. Kuperman, T. Akal: Underwater acoustic communications using time reversal, IEEE-JOE **30**(4), 852–864 (2005)

15.83 J.R. Buck, J.C. Preisig, M. Johnson, J. Catipovic: Single-mode excitation in the shallow-water acoustic channel using feedback control, IEEE-JOE **22**(2), 281–291 (1997)

15.84 J.A. Flynn, J.A. Ritcey, D. Rouseff, W.L.J. Fox: Multichannel equalization by decision-directed passive phase conjugation: experimental results, IEEE-JOE **29**(3), 824–836 (2004)

15.85 S.E. Cho, H.C. Song, W.S. Hodgkiss: Successive interference cancellation for underwater acoustic communications, IEEE-JOE **36**(4), 490–501 (2011)

15.86 C. Petrioli, R. Petroccia, J. Shusta, L. Freitag: From underwater simulation to at-sea testing using the ns-2 network simulator, Proc. OCEANS'11 (2011) pp. 1–9

15.87 J. Heideman, M. Stojanovic, M. Zorzi: Underwater sensor networks: Applications, advances, and challenges, Phil. Trans. R. Soc. **370**, 157–175 (2012)

15.88 D. Pompili, I. Akyildiz: Overview of networking protocols for underwater wireless communications, Communications Magazine, IEEE **47**(1), 97–102 (2009)

15.89 J. Heidemann, W. Ye, J. Wills, A. Syed, Y. Li: Research challenges and applications for underwater sensor networking, Proc. IEEE WCNC, Vol. 1 (2006) pp. 228–235

15.90 M. Chitre, S. Shahabodeen, M. Stojanovic: Underwater acoustic communications and networking: Recent advances and future challenges, Mar. Technol. Soc. J. **42**(1), 103–116 (2008)

15.91 E.M. Sozer, M. Stojanovic, J.G. Proakis: Underwater acoustic networks, IEEE-JOE **25**(1), 72–83 (2000)

15.92 R. Eustice, H. Singh, L. Whitcomb: Synchronous-clock one-way-travel-time acoustic navigation for underwater vehicles, J. Field Robotics **28**, 121–136 (2011)

15.93 M. Stojanovic: Design and capacity analysis of cellular-type underwater acoustic networks, IEEE-JOE **33**(2), 171–181 (2008)

15.94 B. Peleato, M. Stojanovic: Distance aware collision avoidance protocol for ad-hoc underwater acoustic sensor networks, IEEE Commun. Lett. **11**(12), 1025–1027 (2007)

15.95 A. Syed, W. Ye, J. Heidemann: Comparison and evaluation of the T-Lohi MAC for underwater acoustic sensor networks, IEEE J. Sel. Areas Commun. **26**(9), 1731–1743 (2008)

15.96 J. Ahn, A. Syed, B. Krishnamachari, J. Heidemann: Design and analysis of a propagation delay tolerant ALOHA protocol for underwater networks, Ad Hoc Netw. J. **9**(1), 752–766 (2011)

15.97 N. Chirdchoo, W.-S. Soh, K. Chua: RIPT: A receiver-initiated reservation-based protocol for underwater acoustic networks, IEEE J. Sel. Areas Commun. **26**(9), 1744–1753 (2008)

15.98 M.K. Park, V. Rodoplu: UWAN-MAC: An energy-efficient MAC protocol for underwater acoustic wireless sensor networks, IEEE-JOE **32**(3), 710–720 (2007)

15.99 M. Zorzi, P. Casari, N. Baldo, A. Harris: Energy-efficient routing schemes for underwater acoustic networks, IEEE J. Sel. Areas Commun. **26**(9), 1754–1766 (2008)

15.100 D. Pompili, T. Melodia, I.F. Akyildiz: Distributed routing algorithms for underwater acoustic sensor networks, IEEE Trans. Wirel. Commun. **9**(9), 2934–2944 (2010)

15.101 A. Patil, M. Stojanovic: A node discovery protocol for ad hoc underwater acoustic networks, Wirel. Commun. Mob. Comput. **13**(3), 277–295 (2013)

15.102 F. Zorzi, M. Stojanovic, M. Zorzi: On the effects of node density and duty cycle on energy efficiency in underwater networks, Proc. IEEE OCEANS'10 (2010) pp. 1–6

15.103 S. Basagni, C. Petrioli, R. Petroccia, M. Stojanovic: Optimized packet size selection in underwater WSN communications, IEEE-JOE **37**(3), 321–337 (2012)

15.104 D.E. Lucani, M. Stojanovic, M. Medard: Random linear network coding for time division duplexing: When to stop talking and start listening, Proc. IEEE INFOCOM (2009) pp. 1800–1808

15.105 M.S. Rahim, P. Casari, F. Guerra, M. Zorzi: On the performance of delay tolerant routing protocols in underwater networks, Proc. IEEE OCEANS'11 (2011) pp. 1–7

15.106 L.F.M. Vieira, U. Lee, M. Gerla: Phero-trail: a bio-inspired location service for mobile underwater sensor networks, IEEE J. Sel. Areas Commun. **28**(4), 553–563 (2010)

15.107 N. Chirdchoo, W.-S. Soh, K.C. Chua: Sector-based routing with destination location prediction for underwater mobile networks, Proc. WAINA (2009) pp. 1148–1153

15.108 E.A. Carlson, P.-P. Beaujean, E. An: Location-aware routing protocol for underwater acoustic networks, Proc. IEEE OCEANS'06 (2006) pp. 1–6

15.109 B. Chen, D. Pompili: QUO VADIS: QoS-aware underwater optimization framework for inter-vehicle communication using acoustic directional transducers, Proc. IEEE SECON (2011) pp. 341–349

15.110 D. Green: Acoustic modems, navigation aids, and networks for undersea operations, Proc. IEEE OCEANS'10 (2010) pp. 1–6

15.111 M. Stojanovic, L. Freitag, J. Leonard, P. Newman: A network protocol for multiple AUV localization, Proc. MTS/IEEE OCEANS'02, Vol. 1 (2002) pp. 604–611

15.112 N.E. Farr, A.D. Bowen, J.D. Ware, C. Pontbriand, M.A. Tivey: An integrated, underwater optical /acoustic communications system, Proc. IEEE OCEANS'10 (2010) pp. 1–6

15.113 M. Stojanovic, J. Preisig: Underwater acoustic communication channels: Propagation models and statistical characterization, IEEE Commun. Mag. **47**(1), 84–89 (2009)

15.114 E.A. Carlson, P.P.J. Beaujean, E. An: Location-aware source routing (LASR) protocol for underwater acoustic networks of AUVs, J. Electr. Comput. Eng. **2012**, 1–18 (2012)